Quantum particles in fractal external potential

UNIVERSITAT POLITÈCNICA DE CATALUNYA
BARCELONATECH
Facultat d'Informàtica de Barcelona

FIB

Marc Amorós

Thesis supervisor: Grigori Astrakharchik

Abstract

The Schrödinger equation gives us a time evolution of the wave function of a certain quantum system, thus we obtain a mathematical description of this system. This project focuses on solving it numerically, using the exact diagonalization method.

We present an algorithm to solve the time-independent version of the equation efficiently for a particle in a box with different boundary conditions, and a second program that performs a quantum superposition of the stationary states previously computed to obtain the time evolution of the wave function.

Using these two programs, we ran several simulations to obtain the properties of a quantum system exposed to an external potential with a fractal shape. The selected two-dimensional fractal was the Sierpinski carpet.

An analysis of the static and dynamic properties was performed, and we corroborated the existence of an exponential scaling law between the ground-state energy and the iteration of the fractal. We also verified the expected diffusive behavior over time of the mean squared displacement of a particle under this fractal shaped potential.

Our work can be extended by using the presented programs to perform more experiments with different parameters or different external potential shapes. The program can also be fine-tuned to solve other kind of systems.

Resum

L'equació de Schrödinger ens dona una evolució temporal de la funció d'ona d'un sistema quàntic concret, la qual cosa ens permet obtenir una descripció matemàtica d'aquest sistema. Aquest projecte se centra a solucionar aquesta equació de forma numèrica, utilitzant el mètode de diagonalització exacta.

Presentem un algoritme per solucionar la versió independent del temps de l'equació, de forma eficient, per una partícula dins una caixa, amb diferents condicions de contorn. També, un segon programa que realitza una superposició quàntica dels estats estacionaris computats prèviament, per obtenir l'evolució temporal de la funció d'ona.

Utilitzant aquests programes, hem executat diverses simulacions per obtenir les propietats d'un sistema quàntic exposat a un potencial extern amb forma fractal. La fractal de dues dimensions seleccionada per l'estudi és la catifa de Sierpinski.

S'ha elaborat una anàlisi de les propietats estàtiques i dinàmiques, i hem corroborat l'existència d'una llei d'escala exponencial entre l'energia de l'estat fonamental i la iteració de la fractal. També s'ha verificat el comportament difusiu esperat del desplaçament quadrat mitjà d'una partícula sota aquest potencial en forma de fractal al llarg del temps.

El nostre treball es pot ampliar utilitzant els programes presentats per realitzar més experiments amb diferents paràmetres o diferents formes de potencial extern. El programa també es pot ajustar per resoldre altres tipus de sistemes.

Resumen

La ecuación de Schrödinger nos da una evolución temporal de la función de onda de un sistema cuántico concreto, lo que nos permite obtener una descripción matemática de este sistema. Este proyecto se centra en solucionar esta ecuación de forma numérica, utilizando el método de diagonalización exacta.

Presentamos un algoritmo para solucionar la versión independiente del tiempo de la ecuación, de forma eficiente, para una partícula en una caja, con diferentes condiciones de contorno. También, un segundo programa que realiza una superposición cuántica de los estados estacionarios computados previamente, para obtener la evolución temporal de la función de onda.

Utilizando estos programas, hemos ejecutado varias simulaciones para obtener las propiedades de un sistema cuántico expuesto a un potencial externo con forma fractal. El fractal de dos dimensiones seleccionado por el estudio es la alfombra de Sierpinski.

Se ha elaborado un análisis de las propiedades estáticas y dinámicas, y hemos corroborado la existencia de una ley de escala exponencial entre la energía del estado fundamental y la iteración del fractal. También se ha verificado el comportamiento difusivo esperado del desplazamiento cuadrado medio de una partícula bajo este potencial en forma de fractal a lo largo del tiempo.

Nuestro trabajo se puede ampliar utilizando los programas presentados para realizar más experimentos con diferentes parámetros o diferentes formas de potencial externo. El programa también se puede ajustar para resolver otros tipos de sistemas.

Contents

List of Figures

List of Tables

Chapter 1

Context

1.1 Introduction

The investigation world is always closely related to computer science. It is very frequent to solve a problem by modelling it on a computer using a certain programming language, and then making simulations to get a solution.

The physics investigation field highly benefits of this problem-solving approaches, as we find plenty of equations with physical meaning without an exact solution. To fix this, we try to solve them by representing these equations in a discrete and finite space, so our computers can handle it, and then we write algorithms to get approximations of a real solution.

This is an interdisciplinary research project, with an important theoretical part that involves some quantum physics knowledge and a practical part that covers the design and development of algorithms to simulate and solve quantum physics systems.

1.2 Stakeholders

It is important to define the stakeholders of any project, to know who is interested of its development and can benefit from it.

The main stakeholder of this project is UPC physics department, and more concretely Grigori Astrakharchikm, who was the impeller of it, by posting a TFG offer on Racó. This can lead to a scientific publication if interesting results are obtained, that is why it can interest him as a researcher.

As every scientific research project, it increases the knowledge on this field in general. If we write a paper about the steps we followed it can be beneficial for any other researcher of quantum particle systems and their unique properties, even they could try to replicate our

results by real experimentation. So it can be considered that this project benefits all the scientific community in a way, more specifically the physics investigators.

1.3 Theoretical concepts

I will summarize some theoretical concepts that are necessary to understand the rest of this document, so the reader can fully comprehend the aim and objectives of this project.

1.3.1 Quantum mechanics

Quantum mechanics is the theory that describes the physical properties of Nature at the scale of atoms and subatomic particles. When it was first formulated during the early decades of the 20th century, it introduced some ground-breaking concepts, such as energy quantization, the uncertainty of position and momentum of a particle and the wave-particle duality of matter.

In classical physics we have Newton's second law, which given a set of initial conditions makes a mathematical prediction of what path a given physical system will take over time. Its quantum analogous would be the Schrödinger equation, which instead requires a statistical interpretation.

1.3.2 Schrödinger equation

Quantum mechanics tells us how the particles behave over time. This description is done using the Schrödinger equation, which provides the time evolution of the wave function of particles. The wave function, generally represented with the letter Ψ, is a mathematical description of the quantum state of the system, and with it, you can obtain the distribution of probability of the measurements that you can do over this system.

The Schrödinger equation is a differential equation, and has the following form:

$$i\hbar\frac{\partial}{\partial t}\Psi\left(r,t\right)=\hat{H}\Psi\left(r,t\right) \tag{1.1}$$

Here we define the Hamiltonian operator $\hat{H}$, which is an operator corresponding to the total energy of that system, including both kinetic (T) and potential energy (V), and for a single particle it takes the form:

$$\hat{H}=\hat{T}+\hat{V}=-\frac{\hbar^2}{2m}\nabla^2+V\left(r,t\right) \tag{1.2}$$

The kinetic energy in quantum mechanics is proportional to the Laplace operator ∇^2, which is the addition of the second partial derivatives of the wave function. The potential energy is a function of the position of the particle, similarly to the classical case.

For the first problem, we are interested in the stationary properties, so we take the time-independent version of the Schrödinger equation:

$$\hat{H}|\Psi\rangle=E|\Psi\rangle \tag{1.3}$$

When solving it, the set of energy eigenvalues that provides (also called energy spectrum) is the set of possible energies obtained when measuring the system's total energy. Here we are interested in finding the ground state of the system, which is its lowest energy state. Differently from the classical systems where the energy of a single particle at zero temperature is finite due to zero-point motion, this ground state energy is always present in the quantum system, even in absolute zero temperature conditions.

1.3.3 Fractals

A fractal is a subset of the Euclidean space that illustrates a property called self-similarity, which means that appears the same at different scales and exhibits similar patterns at increasingly smaller scales.

1.3.4 Sierpiński carpet

The Sierpiński carpet is a plane fractal that was first described by Wacław Sierpiński in 1916, as a two dimensions generalization of the Cantor set, that was discovered in 1874 by Henry John Stephen Smith and introduced by German mathematician Georg Cantor in 1883.

The Cantor ternary set is created by iteratively deleting the open middle third from a set of line segments.

Figure 1.1: First six steps of Cantor ternary set

To describe fractals properties, we frequently use the fractal dimension, which is a ratio that provides a statistical index that shows how the detail in the pattern of the fractal changes with every iteration. These leaves us with non integer dimensions, as the dimension of the Sierpinski carpet is $log(8)/log(3) \approx 1,8927...$ We can see the first four iterations of the Sierpinski carpet fractal on Figure 1.2.

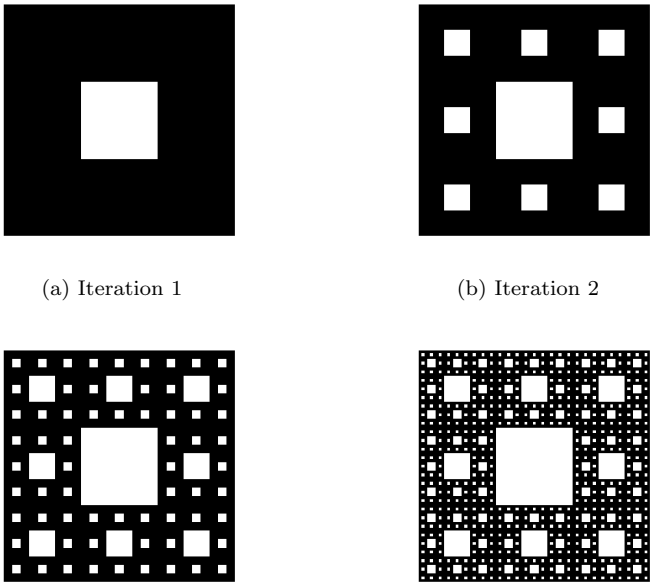

(a) Iteration 1

(b) Iteration 2

(c) Iteration 3

(d) Iteration 4

Figure 1.2: First four iterations of the Sierpinski carpet

Chapter 2

Justification

The interdisciplinary aspect of this project is what attracts me the most. Quantum mechanics is a complicated field that we do not study on the GEI degree. That is why this project really interested me personally, as it gives me the opportunity to learn and work on a subject that is quite different to what I am used to, and I am also able to contribute on a physics research project applying my computation knowledge, something I would enjoy doing as a future job.

There have been recent experiments [1, 2], that have shown how it is possible to produce a Bose-Einstein condensate. In the last few years, new experimental techniques have been developed, and it became feasible to create two-dimensional Fermi or Bose gas in highly controllable external potential. The projected potential can be chosen essentially in any desired shape, fractal shapes included. These means that most of our work could be verified by these experiments. Moreover, we could find some related articles that studied the properties of particles on a fractal environment, but they did not obtain the energetic, structural and dynamic properties as we do.

Chapter 3

Scope

3.1 Objectives

The aim of the project is to study the properties of quantum particles in a fractal external potential. The main goal is to obtain a detailed description of such a system in terms of energetic, structural and dynamic properties. In particular, the energetic properties can be quantified by evaluation of the ground state energy and the excitation spectrum. The structural property of interest is the density profile. The dynamic property to be calculated is the diffusion coefficient.

We consider the external potential in the shape of a Sierpinski carpet. It has a fractal structure, with the fractal dimensionality between 1 (i.e. a line) and 2 (i.e. a plane). The strength of the external potential is considered to be infinite (i.e. hard walls) in the positions where the fractal is present. It means that the particles cannot diffuse freely in the system. At the same time, the phase space is joined, that is the particle is allowed to move between any two points where the external field is absent. The fractal shape is defined in a simple recursive procedure and depends on the recursion level.

One of our goals is to provide a detailed description of the properties of quantum particles in fractal external potential. In particular, we plan to verify the existence of a simple scaling law between the zero-point energy of the system and the number of iterations of the fractal.

This is an interdisciplinary problem, based on application of mathematical concepts to the field of quantum physics, and relies on the use of numerical methods. This project requires carrying out a scientific investigation and a priori it is not clear which method is going to be the best to study these properties.

We plan to execute this study considering two different problems:

1. Solve Schrödinger equation using exact diagonalization of a discretized Hamiltonian
2. Solve the time-dependent Schrödinger equation using superposition of stationary states

3.2 Potential obstacles and risks

The biggest obstacle to me is the fact that I have to really comprehend all the physical concepts to be able to properly implement the techniques to model and solve the quantum systems that we propose. I am a computer science student and I have not been taught quantum mechanics, what means that this project involves a lot of self-studying by my part.

Another risk is the possibility that the system properties that we selected to observe do not present any reasonable pattern, or that we can not see it because of lack of scope. That is why we want to try different experiments and compare the viability of studying different properties.

Together with the previous risk, there is the obvious obstacles that you find in this kind of experiments, related with the lack of realism of a discretized system compared to the real world. This discrete barrier is found by the necessity of modelling the experiments in a finite and computable way, as we also can not be too ambitious with the computational resources needed to obtain a solution.

Chapter 4

Methodology and rigour

4.1 Methodology

As this is a research project, every step we take is going to be vastly justified. The modelling of the quantum system is going to be verified by computing some properties that we know in advance, such as that the ground energy of a particle in a box without an external potential has to be equal to $\frac{\pi^2\hbar}{2mL^2}$. Also, all the techniques followed to model and obtain some properties of it are going to be referenced and explained in detail on the thesis documentation.

My supervisor and I have followed a pretty loose Agile methodology [3], which was decided at the begging of the project. We have a meeting once a week, to review the progress of the project and comment the possible results obtained. We also set goals for the near future, and debate about the path to follow.

On the last three months of the project, Pietro Massignan also joined us on the weekly meetings. He helped us to give physical meaning to the results obtained by our study, together with Grigori. He also participated in the decision-making, the design of the experiments and the process of setting the short term goals to accomplish.

Chapter 5

Time planning

As we can see in FIB's documentation [4], the TFG corresponds to 18 credits, which have a 30 hours workload each. This means that the total hours spend on the project must be of 540 hours.

With this in mind, we plan a working routine of four hours a day, from the 1st of February to the 15th of June 2021, what makes a total of 135 days of work, from Monday to Sunday.

5.1 Project phases

To achieve the aim of the project, that is to study the properties of quantum particles in a fractal external potential, we are going to develop to algorithms two algorithms, one for observing static properties and another to obtain the dynamic ones. This process can be seen as two individual studies, with the respective sections on each one:

- Previous study (PS)
- Design (DN)
- Implementation (IM)
- Data analysis (DA)

5.2 Description of tasks

As I mentioned in the previous section, each of the three methods that we are using is going to follow the phases previously specified. As this is a research project and we do not really know a priori the results that we are going to obtain, we might be changing the order of the tasks. Each task is assigned a different key code to identify it easily.

5.2.1 Project management

Here I specify the tasks that are found in every kind of project that are related with the management of this one. Some of them are done during GEP, such as the definition of the scope, the planning, the budget and the sustainability studies of this project.

The others are executed during the hole project. For example, we planned a weekly meeting with the thesis supervisor to coordinate our work, so he could explain me his ideas about the current state of the project and comment some possible improvements or clarifications about it. In this task it is also included the continuous emails we send each other during the week for possible doubts or some daily details about the progress of my work.

As this is a research project that can possibly end as a scientific publication, we must strictly justify every step we take and keep track of the methodology we are following. This is done within the documentation task, which will we be done during the hole project, as we will update the documentation on every action we perform.

- Scope (T1)
- Planning (T2)
- Budget (T3)
- Sustainability (T4)
- Meetings (T5)
- Documentation (T6)

5.2.2 Building Sierpinski carpet

We have to design and implement a Matlab program that can generate a Sierpinski carpet fractal, given a certain input size and iteration of the fractal. The fractal computed must be stored on a matrix, as we are going to use this program on the other algorithms to generate the external potential shape.

5.2.3 Exact diagonalization method

The following tasks consist on the study of the time-independent Schrödinger equation and the design of how it can be solved for a system composed of a particle in a box and with a certain fractal shaped potential. A study of the possible boundary conditions and its effect on the solution has to be done. The implementation of this design is the following step, and all of this leads us to the possibility of obtaining the energetic and structural properties of the system, such as the ground state energy or the Inverse Participation Ratio. With all these data, we can study the relation it has with the external potential that we applied, and see if we can find a relation with its fractal dimension.

- Previous study (T8)
- Design (T9)
- Implementation (T10)
- Data analysis (T11)

5.2.4 Time-evolution of the wave function

The following tasks are related to the study of the time-dependent Schrödinger equation. In these tasks we have to understand the concept of quantum superposition, to be able to design an algorithm that uses the previous computed possible quantum states of the system, to calculate the time evolution of the wave function given a certain initial state by performing a superposition of all these possible states. This will allow us to study dynamic properties that variate over time, such as the mean square displacement of a particle. It also allows us to generate different time evolutions to properly understand the effect of this fractal shaped external potential on the diffusion of the particle. All the

- Previous study (T12)
- Design (T13)
- Implementation (T14)
- Data analysis (T15)

5.3 Tasks dependencies

The dependencies between tasks are quite trivial, as for the correct development of the two studies, their related tasks have to be done sequentially, in the following order: previous study, design, implementation and data analysis. Maybe some of them can be overlapped, such as design and implementation, as sometimes is better to design one part of the code and implement it, and then go back again to design process.

One clear dependency thought, is the fact that the program for building the Sierpinski carpet (T7) has to be implemented previously to the implementation of the first experiment.

The project management tasks, related with the current state of the project, have no dependencies, as they take place during all the months of the project development.

5.4 Gantt diagram

To properly organize the tasks over time and to specify their duration, we present the information in a Gantt diagram, that you can see on Figure 5.1. The tasks' duration is summarized in the Table 5.1.

Notice how tasks of data analysis have more time assigned, as they include the execution of the different programs, that my vary a lot depending on the program and the iterations that we decide to compute.

There are no time values assigned to the tasks of Meetings and Documentation, as they will occur during all the other tasks, which have an implicit fraction of their dedicated time assigned to these two tasks, as they must be done along with all the project's development.

Id	Task name	Hours
T1	Scope	32
T2	Planning	32
T3	Sustainability	32
T4	Budget	32
T5	Meetings	-
T6	Documentation	-
T7	Building Sierpinski carpet	44
T8	Exact diagonalization: Previous study	44
T9	Exact diagonalization: Design	44
T10	Exact diagonalization: Implementation	44
T11	Exact diagonalization: Data analysis	52
T12	Time-evolution: Previous study	44
T13	Time-evolution: Design	44
T14	Time-evolution: Implementation	44
T15	Time-evolution: Data analysis	52

Table 5.1: Table to test captions and labels

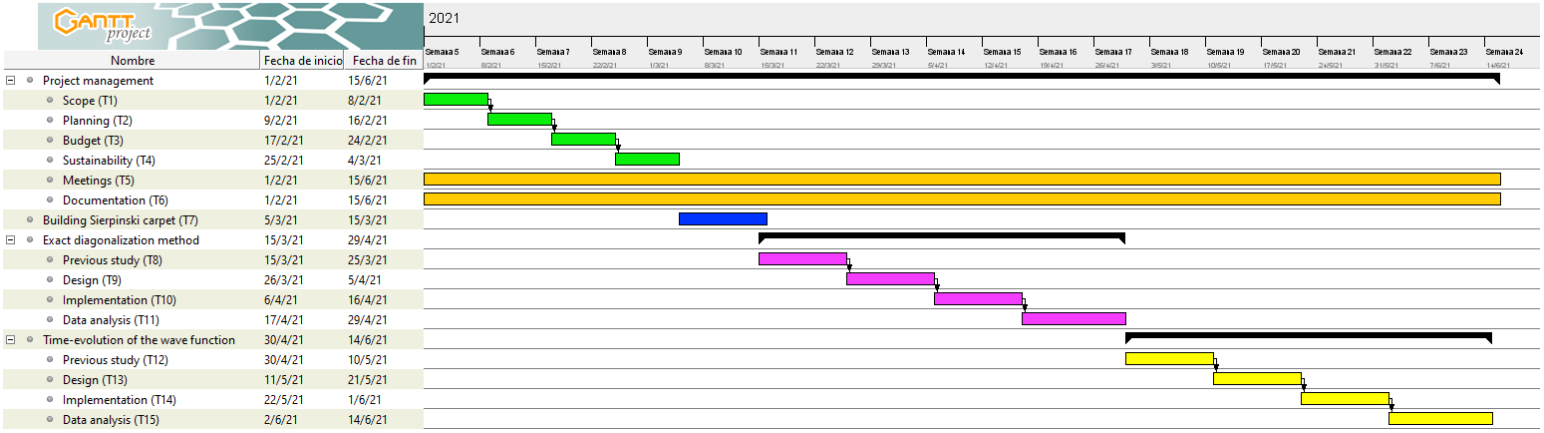

Figure 5.1: Gantt chart of the tasks of the project

5.5 Risk management

There are some implicit risks in every project when you plan it in advance.

The main limitations we can find are about computational cost. We know that exist the algorithms to solve the problems we are tackling, but maybe the cost of solving the systems for a high number of iterations of the fractal is too much for our computers. The more iterations we can do, the more precise our results are going to be. This can lead to a rescheduling of the tasks, as we might need more time to find and implement a more efficient way to solve the equations.

If this happens, we will focus on other related simulations, that also study properties of the Sierpinski carpet fractal, but that do not make use of the diagonalization method, which is where we are most likely to find a computational limit, as we need to find eigenvalues and eigenvectors of pretty big matrices.

Chapter 6

Budget

6.1 Identification of costs

Referent to this project, we can consider three kinds of costs:

- Thesis supervisor: the continuous supervision of a physicist.
- Development: the laptop and the main developer work.
- Server: energy and rental of the servers to run the simulations.

6.1.1 Thesis supervisor

This is an interdisciplinary project which involves a lot of specific quantum physics concepts. That is why there appears the need of a physics PHD to supervise and orientate the project.

We established a weekly meeting of one hour approximately, that takes place every Tuesday. He also keeps track of my developing process and answers my emails during the week, what can be approximated by on hour of work a week as well.

We can see how an investigator at UPC has a monthly salary of 2.313,52€ on the *Taules retributives PDI laboral 2020* [5], which implies a salary of 12,85€/h approximately.

6.1.2 Development

This is an A modality TFG [6], which implies that is being done by a computer engineering student. The economic cost on this process is the usage of his personal laptop, which is a LP gram, that can be found for 1200€ on Amazon [7], and the salary of the developer, which we set to be a standard salary of 9€/hour.

6.1.3 Server

All the simulations are run on a server. Some of the simulations need considerable amount of resources, such as memory. That is why we run them on a server with 16 CPUs and 64GB of RAM, which we could rent online for approximately 270€ per month.

6.2 Cost estimates

The costs of this project are briefly detailed in Table 6.1, which summarizes the human resources costs and Table 6.2, which includes some general costs. All together, leads to a total of 6.798,77€. This cost is divided by tasks on Table **??**. TODO

Profile	Salary	Cost/year	Cost/h	Hours	Cost
Thesis supervisor	32.374,48	42.044,78	16,69	20	333,77
Developer	-	-	9	450	4.050
Total					4.383,77

Table 6.1: Human resources costs

Concept	Quantity	Cost
Developer laptop	1	1.200
Server	4,5	1.215
Total		2.415

Table 6.2: Resources costs

6.3 Management control and contingency plan

We have included a contingency based on the renting of the servers for the whole duration of the project, even though we are only going to use them once the development process is done.

In case of possible errors on the prediction of costs, we will add a contingency margin of 10% for human resources costs and generic costs. This equals to an added cost of 679,88€, and leads to a total budget of **7.478,65€**.

Chapter 7

Sustainability

7.1 Reflection

I have been aware for years that computer science can have a negative and positive impact on people's lives, on the environment and on the world in general. That's why I try to always think about the ethic consequences of my actions and not waste resources both in my particular life and on any kind of project I am involved on. I find that society does not give the social and environmental sustainability of projects the importance it deserves.

In any project it is important to perform a sustainability analysis considering three dimensions: economic, environmental and social.

7.2 Economic dimension

The different aspects of the economic dimension of this project are:

- This project has a really reduced budget, as the main developer is a student.
- We have established some strategies to entirely organize this project online, so we do not need any kind of office, what could be and additional cost.
- We could analyze the need of the renting of the server for the entire duration of the project, but as this is a research project we are not sure about how long we are going to need it. If we finish earlier we can always stop paying it.

7.3 Social dimension

We state some aspects of the social dimensions as follows:

- If we end up with interesting results, it is very likely that this project evolves in a scientific publication. These means that it contributes to the scientific knowledge as it is a research field that has not been properly explored yet.

- Our work can lead to other people getting interested in the study of the behaviour of quantum particles in a different shaped external potentials.
- It can also demonstrate and show off how important and successful an interdisciplinary project can be, something really important in a bast range of fields.

7.4 Ambiental dimension

To end up with our sustainability analisis, we explore the abiental aspects of the project:

- The resources used to develop this project are the ones stated previously, we do not extract or use any kind of natural resource. We also do not emit or produce anything harmful for the environment.
- We do not waste office supplies and we try to cut down to the minimum the amount of it that we use.
- The programs that we run on the server are really optimized, to save computation time, and with it, energy.

Chapter 8

Generating Sierpinski carpet

The first program we designed is a Sierpinski carpet fractal generator. These means that, given two inputs N and *iter* it returns a matrix of size $N \times N$ that contains a Sierpinski carpet at the *iter* iteration. An example can be found on Figure 8.1, where this fractal would be the output matrix with the parameters $iter = 3$ and $N = 27$. On this figure, the values of the matrix that contain a 0 or a 1 are represented by a black or white pixel respectively.

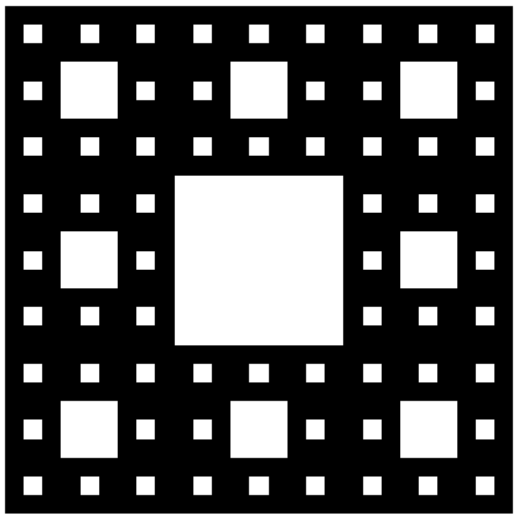

Figure 8.1: Sierpinski carpet of iteration 3

It is important to mention that, because of the nature of the Sierpinski carpet, we only can perform calculations for values of N that are positive multiples of 3^i, being i the iteration

of the fractal that we are using as the shape of the external potential energy.

$$N = 3^i k \qquad k \in \mathbb{N}^+ \tag{8.1}$$

This is quite intuitive to understand, as for example, you can not map a proper Sierpinski carpet of iteration 1 (example on Figure 1.2.a) on a matrix of shape 10×10 as 10/3 does not give you an integer solution, and you would obtain a non-symmetrical and degenerate fractal.

Once we had these limitations in mind, we developed a recursive algorithm to know if each position of the matrix has to be filled with a one or a zero. We implemented it with Matlab, as we are going to use it as a module that we will call from other Matlab scripts. This program will call the method *isSierpinskiCarpetPosFilled* for each position of a $N \times N$ matrix, with the parameter $d = iter - 1$.

Algorithm 1 isSierpinskiCarpetPosFilled(x, y, width, height, d)

Require: $mod(N, 3^{iter}) == 0$

```
1:  x2 = floor(x * 3 / width)
2:  y2 = floor(y * 3 / height)
3:  if x2 == 1 and y2 == 1 then
4:      return 1
5:  end if
6:  if d > 0 then
7:      x = x - floor((x2 * width + 2) / 3)
8:      y = y - floor((y2 * height + 2) / 3)
9:      width = floor((width + 2 - x2) / 3)
10:     height = floor((height + 2 - y2) / 3)
11:     return isSierpinskiCarpetPosFilled(x, y, width, height, d - 1)
12: else
13:     return 0
14: end if
```

The pseudocode of the algorithm (1) is a bit obfuscated, but I am going to break it down.

On line 3, we can see one of the base cases. This is when the pixel is placed in the center of the square, which is always filled, so we return a 1. The condition is making sure that the position (x, y) is within the center square, which is the middle section of dividing the X and Y coordinates by three.

The next base case is the else from line 13, where you enter when you have not "found" a center square, as the iteration parameter is two small, so you return a 0. On a theoretical fractal of infinite iterations, you would never enter this condition.

The last section is the recursive one, that starts at line 6. Here we make some reshape to the position of the pixel and the width and high variables, to reduce the problem to a fractal of one third of size. This can be seen as a zoom in into the area that our pixel (x, y) is placed, and now we can check if it is in the center of this smaller box, or otherwise we have to keep iterating until we find it or until we reach the depth limit.

Chapter 9

Stationary properties of a quantum particle in Sierpinski carpet

As our goal is to study the effect of the external potential field on a quantum system, we are going to compute the ground state energy of the quantum system that we present. To do so, we have to solve the time-independent Schrödinger equation numerically for one particle. We can see on section 10.1 how this equation can be obtained from the original Schrödinger equation.

$$\hat{H}|\Psi\rangle = E|\Psi\rangle \tag{9.1}$$

9.1 Boundary conditions

First, we have to define the boundary conditions of the box we place the particle in.

9.1.1 Zero boundary conditions

One possibility is to impose zero boundary conditions (z.b.c.) by defining a box with a side length of L= 1 centered at the origin and apply Dirichlet boundary conditions that define a value of the solution $f(x, y) = 0$, on the border area. Physically, such conditions correspond to a hard wall of an infinite size, so that the particle cannot escape the box.

A single quantum particle in a box with zero boundary conditions and without any potential energy has a finite energy equal to

$$E_{box,zbc} = \frac{\pi^2\hbar^2}{mL^2} \tag{9.2}$$

9.1.2 Periodic boundary conditions

Another possibility is to use periodic boundary conditions (p.b.c.). In this case we use a box with a side length of $L = 1$ centered at the origin and we apply Neumann boundary conditions, defining the partial derivatives equal to zero at the border of the box:

$$\frac{\partial}{\partial x} f(x = L/2, y) = 0 \tag{9.3}$$

$$\frac{\partial}{\partial y} f(x, y = L/2) = 0 \tag{9.4}$$

Conditions (9.3-9.4) are equivalent to periodic boundary conditions.

Physically, periodic boundary conditions provide a faster convergence to the thermodynamic limit when the box size is increased. Indeed, for any box size L, the ground-state energy of a single particle in a box without potential energy is equal to its thermodynamic value,

$$E_{box,pbc} = 0 \ , \tag{9.5}$$

contrarily to $1/L^2$ dependence observed in the case of zero boundary conditions (9.2). Excitation spectrum in a box with periodic boundary conditions is $E_{n_x,n_y} = \frac{2\pi^2\hbar^2(n_x^2+n_y^2)}{mL^2}$ where $n_x = 0; \pm 1; \pm 2; \cdots$ and $n_y = 0; \pm 1; \pm 2; \cdots$ are quantum numbers of excitations along two directions.

9.2 Discretize the Hamiltonian operator

From equation (9.1), we can see how if we define the Hamiltonian operator $\hat{H}$ in a matrix form, we can solve it by finding the eigenvalues and eigenvectors of it, as E are the eigenvalues of Ψ when $\hat{H}$ act on Ψ. This is also called the diagonalization method.

$$\hat{H} = \hat{T} + \hat{V} = -\frac{\hbar^2}{2m}\nabla^2 + V \tag{9.6}$$

To simplify the calculation, we are going to leave our results in function of $-\frac{\hbar^2}{2m}$. So we are left with the Laplace operator ∇^2 and the potential V. The Laplace operator acting on a function f is equal to the sum of the second derivatives of f. We are going to solve this equation in a discrete space, and the multidimensional discrete Laplacian operator is a Kronecker sum of the one dimensional discrete Laplacians, so first we have to obtain this discrete derivatives for each dimension.

The fact that our space is discretized means that we have N different possible values for the x coordinate. We are going to define x_i as the i th value of x, for $1 \leq i \leq N$.

Now, using the finite-difference method, we can define a second derivative of a function f like:

$$f_i = f(x_i) \tag{9.7}$$

$$\frac{\partial^2 f}{\partial x_i^2} \approx \frac{f_{i-1} - 2f_i + f_{i+1}}{\Delta x^2} \tag{9.8}$$

As we want to solve this problem for a particle on the plane, the Hamiltonian operator has 2 dimensions. The Kronecker sum of two discrete Laplacians is defined as:

$$\mathbf{L} = \mathbf{D_{xx}} \oplus \mathbf{D_{yy}} = \mathbf{D_{xx}} \otimes \mathbf{I} + \mathbf{I} \otimes \mathbf{D_{yy}} \tag{9.9}$$

where $\mathbf{D_{xx}}$ and $\mathbf{D_{yy}}$ are one dimensional discrete Laplacians in the x and y-directions correspondingly, and $\mathbf{I}$ is the identity matrix of appropriate size.
Looking at equation (9.8), we can define the one dimensional discrete derivative of x ($\mathbf{D_{xx}}$) as follows:

$$\mathbf{D_{xx}} = \frac{1}{\Delta x^2} \begin{pmatrix} -2 & 1 & & & \\ 1 & -2 & 1 & & \\ & \ddots & \ddots & \ddots & \\ & & 1 & -2 & 1 \\ & & & 1 & -2 \end{pmatrix} \tag{9.10}$$

This representation of the derivative is done by applying zero boundary conditions to the box.

Periodic boundary conditions can be as well imposed in the discrete form. In this case, matrix $\mathbf{D_{xx}}$ has two additional elements on positions $(N, 1)$ and $(1, N)$:

$$\mathbf{D_{xx}} = \frac{1}{\Delta x^2} \begin{pmatrix} -2 & 1 & & & 1 \\ 1 & -2 & 1 & & \\ & \ddots & \ddots & \ddots & \\ & & 1 & -2 & 1 \\ 1 & & & 1 & -2 \end{pmatrix} \tag{9.11}$$

Now, defining $\mathbf{D_{yy}}$ the same way as $\mathbf{D_{xx}}$ but with Δy^2, we can compute the discrete Laplacian as the matrix $\mathbf{L}$ and define the Hamiltonian in a matrix form.

$$\nabla^2 \approx \mathbf{L} \tag{9.12}$$

$$\mathbf{L} = \mathbf{D_{xx}} \oplus \mathbf{D_{yy}} \tag{9.13}$$

The potential can easily be represented in a matrix form by generating a Sierpinski carpet of the size of our box. Then we store a matrix with the information if each point of our discrete space has zero value of the potential or not.

$$\mathbf{H} = \mathbf{L} + \mathbf{V} \tag{9.14}$$

$$\mathbf{L}\psi + \mathbf{V}\psi = \mathbf{E}\psi \tag{9.15}$$

Now, we end up solving the equation (9.15) by diagonalization of $\mathbf{H}$ matrix and find its eigenvalues and eigenvectors. The obtained solutions describe the ground state and excited states of the single-particle problem. The ground-state energy and wave function correspond to the eigenvalue with the lowest value and its eigenvector.

9.3 Finding eigenvalues and eigenvectors

We have reduced the original problem of finding the spectrum of a quantum particle in a fractal external field to a well known problem of numerical calculus and by extension computer science: finding the eigenvectors and eigenvalues of a matrix. There are numerous methods and algorithms that allow to solve this problem, and selecting the optimal one was of major importance, as the execution time of different algorithms varies greatly.

Our program that solved the previously explained problem was implemented using Matlab programming language, as we had some previous knowledge of it, and it gives a lot of facilities for mathematical problem-solving. One example is the method *eigs*, which can compute the N smallest eigenvalues of a matrix. This method was really useful for the initial prototypes of the project, as it makes it really easy to compute the smallest eigenvalue and its corresponding eigenvector of any matrix.

But we quickly realized that for larger matrices, it performed way worse. Then tried to use another algorithm to obtain the eigenpairs in less time. We made some research on the best possible methods, and we decided to try an algorithm called *Locally Optimal Block Preconditioned Conjugate Gradient (LOBPCG)*. This is a matrix-free algorithm, which means that it does not store the matrix on memory, but accesses it by evaluating matrix-vector products. This method is preferable when the matrix is huge and storing and manipulating it would cost a lot of memory and computing time. The algorithm assumes that the matrix is symmetric and positive-definite. From equation (9.10) and equation (9.11) we can see how the matrix that we want to know its eigenpairs of is symmetric, in both boundary conditions. We also know that it is positive-definite in both cases, as it can be seen how both matrices satisfy the following properties:

- All their eigenvalues are real and positive, as there can not be an estate of the system with 0 or negative energy.
- They are congruent with a diagonal matrix with positive real entries.
- All their leading principal minors are positive.
- There exists an invertible matrix B with conjugate transpose B^* such that $M = B^*B$.

We found an implementation of this algorithm for Matlab [**?**] and Octave [**?**], and we performed some experiments to see how both methods performed.

In Figure 9.1 we show how computing just the smallest eigenvalue is drastically faster with the LOBPCG algorithm. This is useful to know, as for the experiments where we just need to obtain the ground state, this algorithm is going to be much faster.

On the other hand, in figure 9.2 it can be seen how computing more than one eigenpair of the matrix is performed way faster with the ***eigs*** method of Matlab. These result is important to know for the problem of knowing the time-evolution of our system, as we need to compute numerous states to achieve precise results.

Another interesting advantage of the LOBPCG algorithm is that we can set the precision that we want for the obtained solution. This is really useful for us, as we might need a lot of precision for small matrices, but we can accept a bigger error margin on larger matrices, what speeds up the computation drastically, as seen on Figure 9.3.

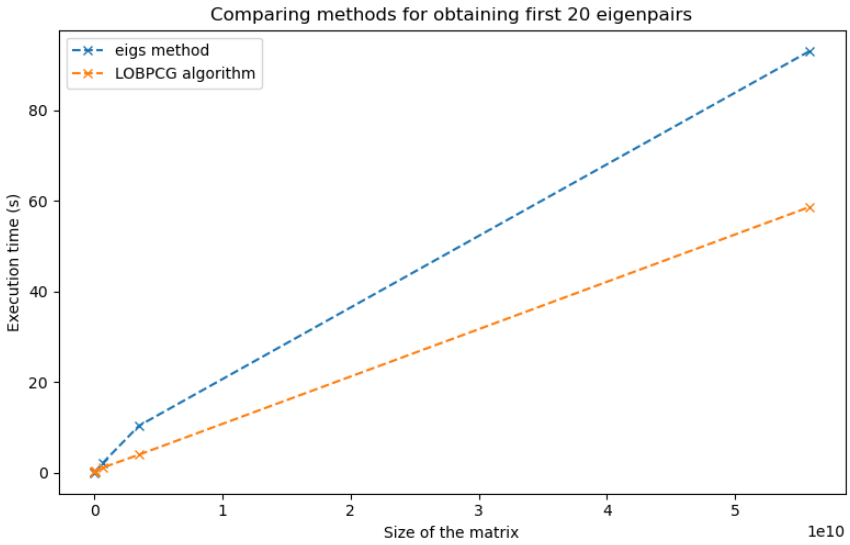

Figure 9.1: Comparing execution time of different algorithms to obtain the smallest eigenvalue

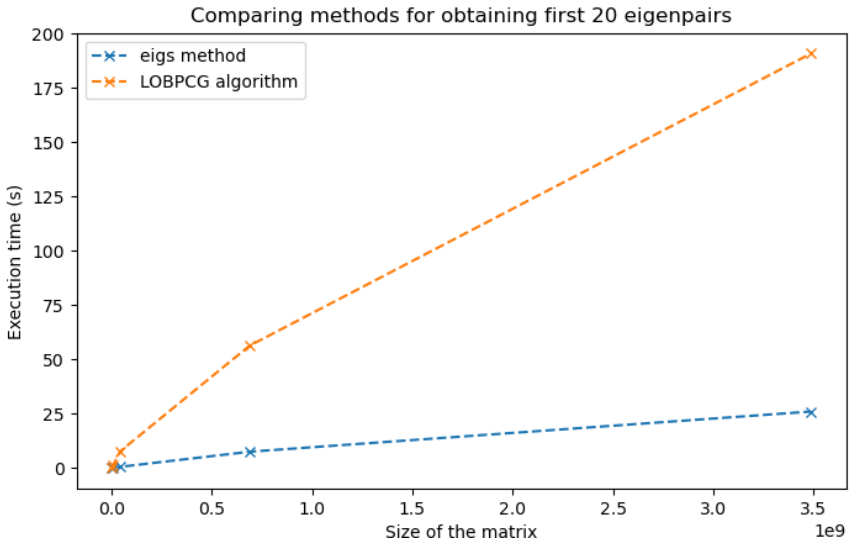

Figure 9.2: Comparing execution time of different algorithms to obtain the 20 smallest eigenvalues

9.4 Normalization

The physical problem of finding the wave functions $\Psi(\mathbf{r})$ and energies of the ground and excited states of the Hamiltonian describing a single particle in a fractal field is interpreted mathematically as a mathematical problem of diagonalizing a matrix and finding its eigenvectors f_i and eignennumbers. This is achieved by discretizing the wave functions

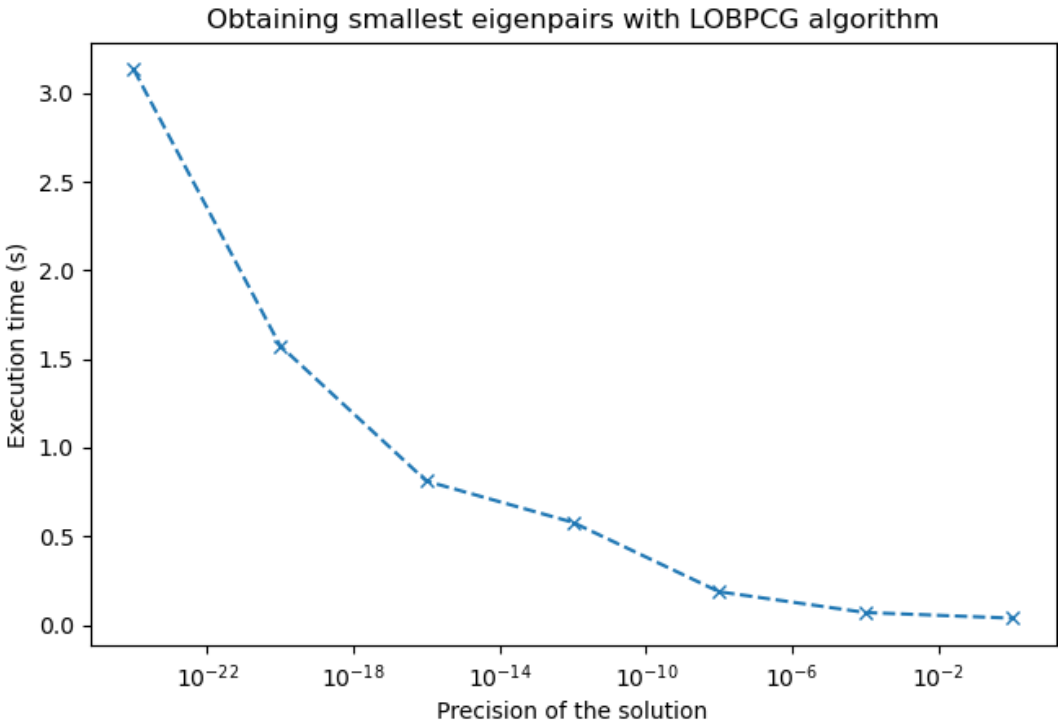

Figure 9.3: Semilog chart of the execution time of computing the smallest eigenpair with $N = 3^5$

$\Psi(\mathbf{r}) \to f_i$.

Different communities use slightly different definitions for the normalization. That is the "physicists" choice is written in terms of an integral as

$$\int |\Psi(\mathbf{r})|^2 d\mathbf{r} = 1. \tag{9.16}$$

Instead the "mathematician" choice involves a summation

$$\sum_i |f_i|^2 = 1. \tag{9.17}$$

In the descretized model, both normalizations are proportional one to the other,

$$\int |\Psi(\mathbf{r})|^2 d\mathbf{r} = \int |\Psi(x,y)|^2 dxdy = \sum_i |f_i|^2 \Delta x^2, \tag{9.18}$$

with the coefficient proportionality given by the discretization area $d\mathbf{r} = \Delta x^2$.

Obviously, each one of the normalizations (9.16) or (9.17) can be used, as long one is done consistently.

9.5 Efficiency of obtaining the ground state energy

An important quantity we want to obtain is the ground state energy of the system. As mentioned previously, this is the energy of the lowest-energy state, and it can be found by performing the discretization of the space and by computing the smallest eigenvalue of the matrix obtained as a result of discretizing the Hamiltonian operator (Equation 9.14).

As the computational resources are finite, the phase space has to be described by a finite grid in order to be represented on a computer. This lattice space (or grid) is represented in a matrix of size $N \times N$. To discretize the Hamiltonian operator, we perform a Kronecker sum of two discrete Laplacians (9.9) corresponding to the kinetic energy of a particle in two dimensional place, (x, y). The Kronecker product of two $N \times N$ matrices produces a resultant matrix of size $N^2 \times N^2$. This is important to notice, as it means that the size of the matrix that represents the discretized Hamiltonian operator increases drastically when we want to improve the precision of our results by increasing the size of the lattice space. Obviously we want to have the most precise results as possible. This means that we have to push our algorithm to the limit and try to compute the results with the biggest lattice space that the execution time of the eigenvalue obtaining process lets us.

Eventually we are interested in the value of the ground state energy in a continuous space, or analogously in the limit, when N, the parameter that defines the discretization size, tends to infinity. To do so, we computed the ground state energy for different values of N and then we interpolated the energy with a quadratic function, to obtain the result when $1/N = 0$.

We illustrate how this method works in Figure 9.4 which shows the ground-state energy computed with different values of N (crosses). We fit the obtained data with a polynamial function and extrapolate the ground state energy when the N tends to infinity. That is, we extract the value of our fit in $x = 0$ point corresponding to $1/N \to \infty$. For example, in the shown case, the ground state energy equals to $529.67\frac{\hbar^2}{2m}$.

Notice that, as we mentioned in section 8, the value of the linear grid size N has to be a multiple of 3^i, being i the iteration of the Sierpinski fractal (see Equation 8.1). This restriction is quite important, as it implies that the matrix that describes the problem increases significantly when simulating higher iterations of the fractal, as the minimum value of N has to be 3^i. To visualize this effect, we added some examples in Table 9.1, where we can see that the minimum value that N can take to simulate an external potential with a Sierpinski carpet of iteration 7 is $N = 2187$, which means we will have to find the eigenvalues of a matrix of size $4.782.969 \times 4.782.969$.

Iteration	Possible N values
1	3, 6, 9, 12, 15, ...
2	9, 18, 27, 36, 45, ...
3	27, 54, 81, 108, 135, ...
4	81, 162, 243, 324, 405, ...
5	243, 486, 729, 972, 1215, ...
6	729, 1458, 2187, 2916, 3645, ...
7	2187, 4374, 6561, 8748, 10935, ...

Table 9.1: The values that N can take for different iterations of the Sierpinski carpet

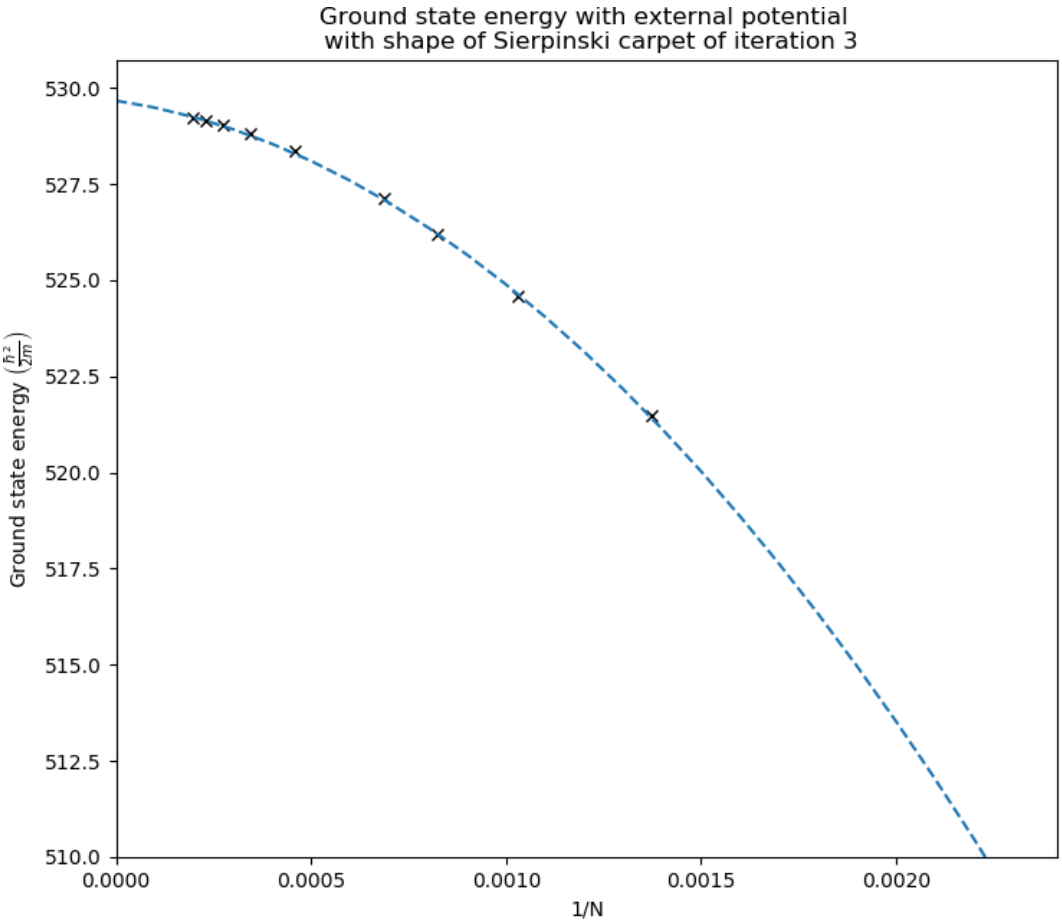

Figure 9.4: Ground state energy and its interpolation to the infinitely-small discretization for Sierpinski carpet of iteration 3. Horizontal axis shows $1/N$ where N is the number of grid points. Crosses, results of the exact diagonalization. Dazed line, parabolic fit of the obtained data.

As the computational cost increases exponentially with the iteration of the fractal, we are going to quickly find a computational limit when trying to compute the zero-point energy for higher iterations.

9.6 Ground-state energy for different iterations of the fractal

One of our initial goals is to verify the existence of a simple scaling law between the zero-point energy of the system and the number of iterations of the fractal. To do so, we compute the ground state energy of the system for each iteration of the fractal. We do it for a number of N values, and use the procedure illustrated in Figure 9.4 to obtain the ground-state energy in a continuous space. The obtained values are reported in Table 9.2

Iteration of the fractal	Ground state energy $\left(\frac{\hbar^2}{2m}\right)$
1	38.59
2	112.78
3	529.43
4	3999.03
5	27387.51
6	107871.18

Table 9.2: Ground-state energy of the system for different iterations of the external potential fractal shape

We are able to perform the extrapolation of the ground-state energy to the continuum limit for iterations from 1 to 6 as the values of N that we had to compute are still computationally manageable (refer to Table 9.1). These computations were done under a zero boundary conditions regime. For larger iteration numbers, we were not able to do a precise interpolation of the value of the ground state energy when N tends to infinity due to limitations of CPU time and memory.

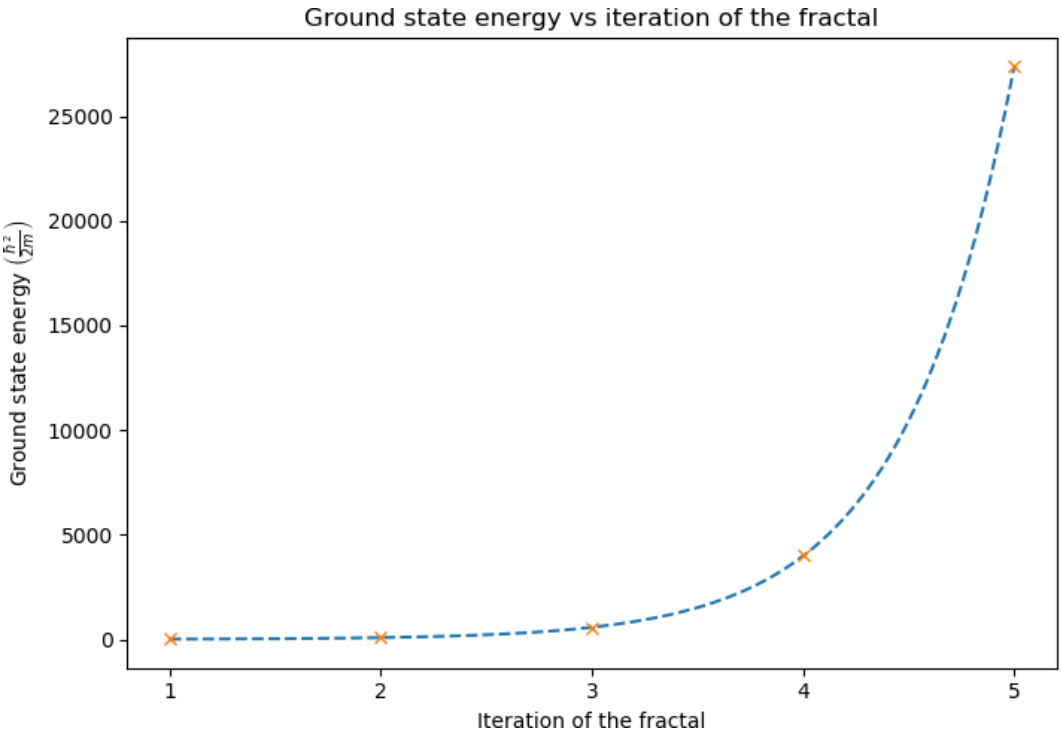

Figure 9.5: Ground state energy of the system for different iterations of the external potential fractal shape.

The obtained results for the ground-state energy are shown in Figure 9.5 as a function of the iteration number of the fractal. As can be seen, the energy increases very fast. In order to demonstrate the the increase in the energy follows an exponential law, we show the same

data on a semi-logarithmic scale in Fig. 9.6. The first five iterations of the fractal clearly follow an exponential scaling law seen as a straight line in this semi-logarithmic plot. To demonstrate it more precisely, we fit the data with an exponential law,

$$y = 1.79 \times e^{1.93x} \tag{9.19}$$

shown with a dashed line.

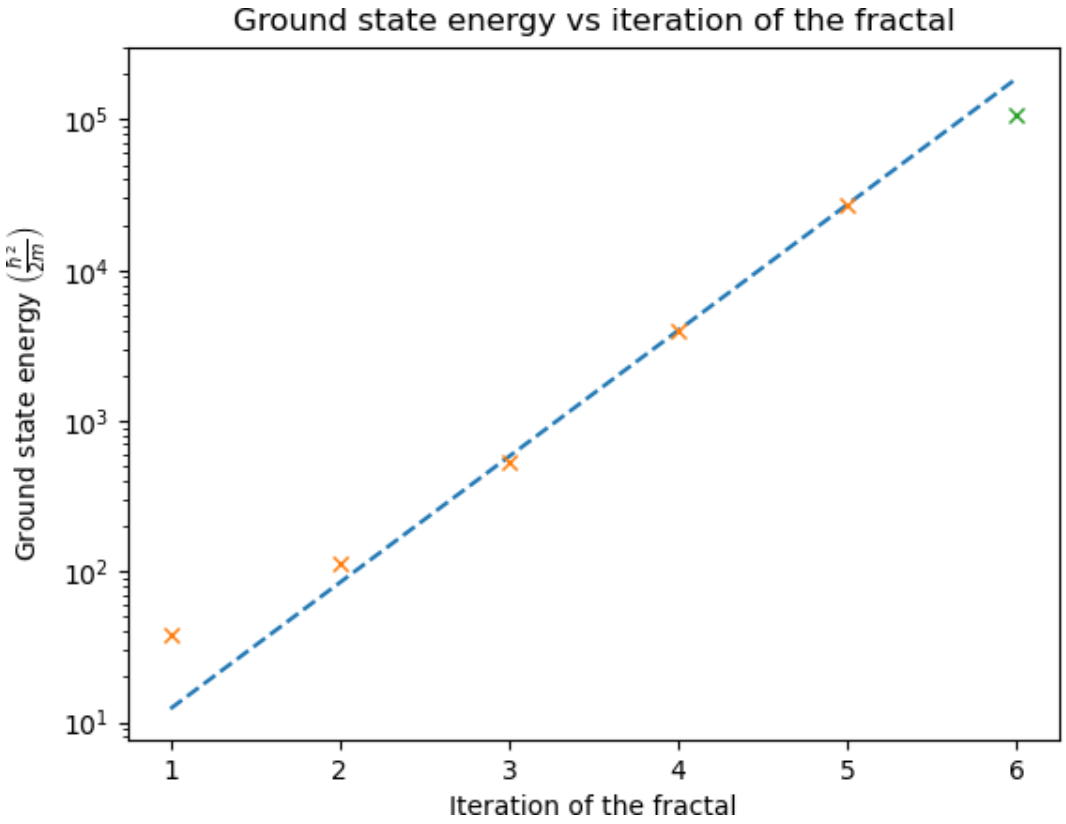

Figure 9.6: Ground-state energy in the continuum limit for different iterations of the external potential fractal (semi-log scale). Red crosses, results of the extrapolation to continuum. Blue dashed line, exponential fit (9.19)

At the same time, we observe that the value of the ground-state energy for iteration 6 does not follow the exponential behavior. The few values that we could compute for iteration 7 seemed to tend to a smaller value than what we would expect if we supposed that all the iterations follow this exponential law.

A possible explanation is the lack of precision for the large iteration numbers, as it becomes notoriously difficult to perform the extrapolation.

9.7 Degenerate eigenvectors

In a quantum system, thre might be two or more quantum states having the same energy. When this happens, such energy level is called a degenerate level and one says these quantum states are degenerate. This happens when the Hamiltonian has more than one linearly independent eigenstate with the same energy eigenvalue.

Seeing this in a mathematical way, we could present the possible eigenvectors of the system as follows:

$$\hat{H}|\psi_i\rangle = E_i|\psi_i\rangle. \tag{9.20}$$

The action of the Hamiltonian $\hat{H}$ to a state $|\psi_i\rangle$ can be interpreted in vector form as some rotation and stretching of the vector,

$$|\psi'\rangle = H|\psi\rangle. \tag{9.21}$$

If the vector $|\psi\rangle$ is an eigenvector, its direction is not changed so that $|\psi'\rangle$ and $|\psi\rangle$ are parallel,

$$\frac{\langle\psi'|\psi\rangle^2}{\langle\psi'|\psi'\rangle\langle\psi|\psi\rangle} = 1 \tag{9.22}$$

and the change in the normalization is governed by the eigenvalue E,

$$\frac{\langle\psi'|\psi'\rangle}{\langle\psi|\psi\rangle} = E^2 \tag{9.23}$$

In the case when several eigenvalues are degenerate, for example $E_0 = E_1 = E_2 = E_3$, any linear combination of corresponding eigenvectors such as $|\psi\rangle = C_0|\psi_0\rangle + C_1|\psi_1\rangle + C_2|\psi_2\rangle + C_3|\psi_3\rangle$, where $C_0, \cdots, C_3$ are some coefficients, is again an eigenvector, i.e. $\hat{H}|\psi\rangle = E_0|\psi\rangle$.

If some vector is "almost" an eigenvector, $|\psi'\rangle \approx H|\psi\rangle$ its direction will almost remain the same, i.e.

$$\frac{\langle\psi'|\psi\rangle^2}{\langle\psi'|\psi'\rangle\langle\psi|\psi\rangle} \approx 1 \tag{9.24}$$

and the change in the normalization will be almost the eigenvale E,

$$\frac{\langle\psi'|\psi'\rangle}{\langle\psi|\psi\rangle} \approx E^2 \tag{9.25}$$

In our system, we find plenty of degenerate states, for the reasons of symmetry. One clear example are the four eigenvectors that its corresponding energy is the ground state energy. Indeed, while Sierpinski pattern has a fractal structure, and might look as being almost random, in reality it has certain symmetries. For example, the Sierpinski pattern reproduces itself when subjected to rotation by 90°, 180° and 270°. As a result, a localized eigenstate might be four-fold degenerate, as other three states obtained by rotation are also eigenstates and have exactly the same energy. Indeed, this is the case for the lowest energy states as shown in Figure 9.8. The diagonalization method in this case might find a linear superposition of the degenerate states. This does not affect the eigenenergies but potentially might result in a very different inverse participation ratio, which is very sensitive to a spatial spreading of a state.

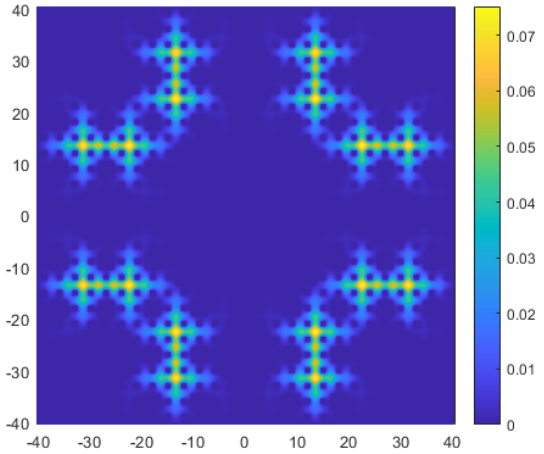

Figure 9.7: Ground state wave function obtained by the diagonalization method without adding noise to the potential.

We have verified that, in the case of the lowest four states, the direct output of the diagonalization method does not correspond to localized states themselves but rather to a linear combination of them, as it can be seen how Figure 9.7 is a linear combination of the four states of Figure 9.8. Furthermore, we were able to find such linear combination of the output of the diagonalization scheme that it restores the localized states.

Although it was easy to find it in the case of the lowest states, it is desirable to lift the degeneracy so that the problem can be entirely avoided. A possible way to do so is to add a weak random potential so that now each localized state will have slightly different energy. In this case, the diagonalization method correctly finds the localized states. We can see the effect of this method on Figure 9.9, where we add a random value in the range $[-\alpha/2, \alpha/2]$ to every position of the fractal potential, breaking the degenerate states. It is important, to select an α value that does not change the spectrum too much, as it can be seen on the figure that for $\alpha = 0.2$ the gap between bands is no longer obvious.

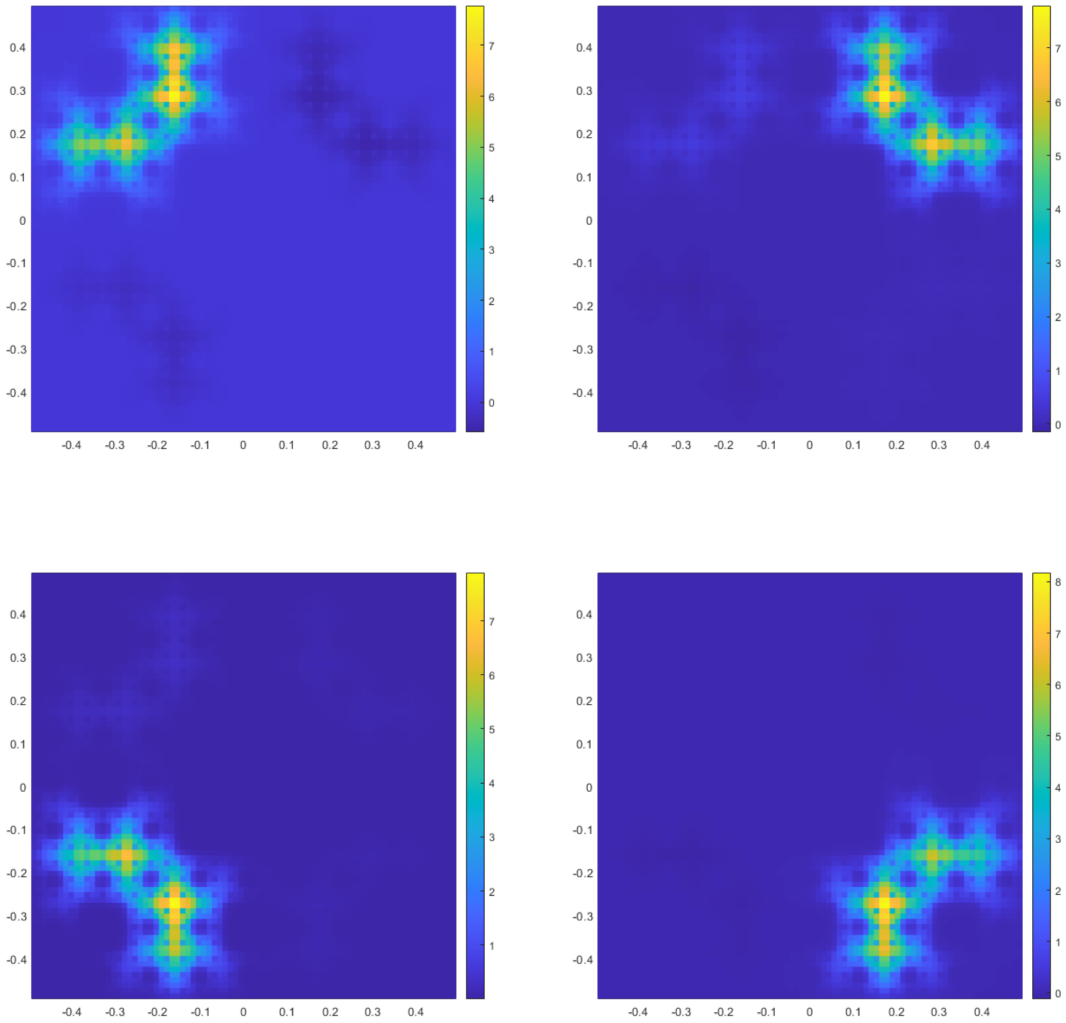

Figure 9.8: Wave function of the four lowest degenerate eigenstates of the system, with zero boundary conditions and iteration 4 of the fractal.

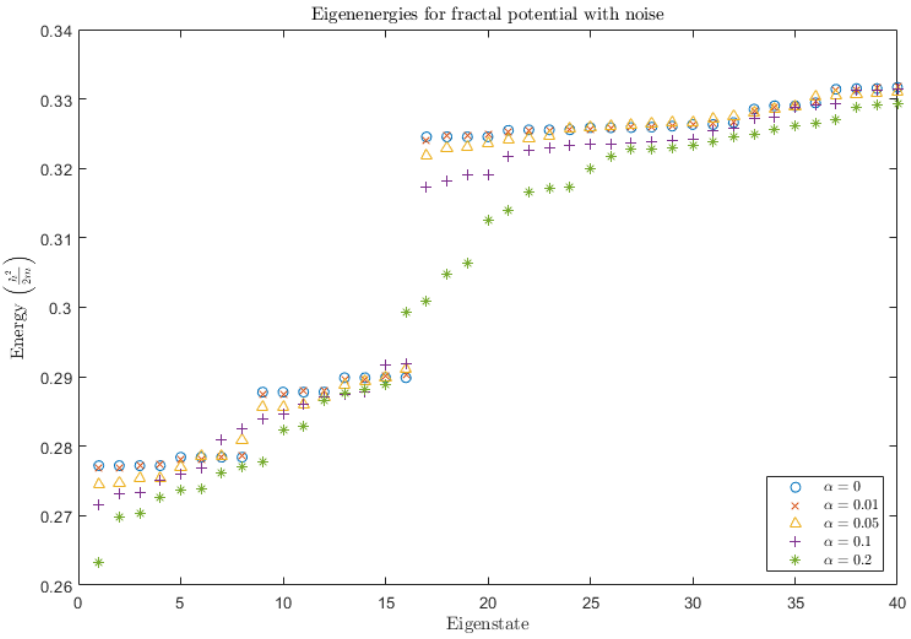

Figure 9.9: Eigenvalues of the system with fractal shaped potential of iteration 4 and zero boundary conditions, with nose of different amplitudes α.

9.8 Inverse Participation Ratio (IPR)

The previous sections were devoted to the energetic properties in the ground state of the fractal. In this section, we focus on the spatial features of the wave functions that we obtain for the different eigenstates.

We find that, for the lowest-energy states, the wave function tends to be localized. In order to interpret the shape of these wave functions we compare them with the shape of the external potential shown in Figure 1.2. Obviously, the wave function has zero value in the areas where there infinitely-high potential Sierpinski carpet is present. At the same time only small fraction of the rest of the available phase space is occupied in the lowest excited states.

In order to discern localized and delocalized eigenstates, we use the Inverse Participation Ration (IPR). In Quantum Mechanics this quantity is often used in order to distinguish a localized state (for example, a bound electron) or an extended state (for example, a delocalized electron). If p_i denotes the probability of finding the particle in state i, then the Inverse Participation Ratio is defined as

$$\text{IPR} = \frac{1}{\sum p_i^2} \tag{9.26}$$

If the particle is localized only in one state, i.e. $p_i = 1$ for that state, then IPR = 1. If the particle is distributed equally between N states, then $p_i = 1/N$ and IPR = N. For our use it is convenient to recast IPR (9.26) in terms of the wave function ψ.

The probability density function of a particle is equal to the square of the absolute value of the wave function at each point. Equation (9.27) shows it for continuous space and equation (9.28) for discrete space.

$$P_{a \leq x \leq b}(t) = \int_a^b |\Psi(x,t)|^2 dx \tag{9.27}$$

$$\Pr(x,t) = |\Psi(x,t)|^2 \tag{9.28}$$

To be a valid probability distribution, one first has to normalize the wave function, i.e. to make sure that the sum of the density on every point adds up to 1.

$$\int_{-\infty}^{\infty} |\Psi(x,t)|^2 dx = 1 \tag{9.29}$$

In terms of the wavefunction, the IPR is defined as

$$\mathcal{R}_q = \frac{\int |\Psi(\mathbf{r})|^{2q} d\mathbf{r}}{\int |\Psi(\mathbf{r})|^2 d\mathbf{r}} \tag{9.30}$$

with $\mathbf{r} = (x, y)$ being a point in the two-dimensional phase space and $d\mathbf{r} = dx\ dy$. In the following we will consider $q = 2$.

Suppose that the particle is in the maximally extended state which uniformly occupies the whole volume $V = L \times L$, that is $\psi = 1/\sqrt{V} = 1/L$ then the inverse participation ratio is $\mathcal{R}_2 = 1/L^2$. If, instead, the particle is localized in a state of size $V = \ell \times \ell \ll L \times L$, then $\psi = 1/\ell$ in that region and $\psi = 0$ otherwise. In that case $\mathcal{R}_2 = 1/\ell^2 \gg 1/L^2$. In other

words, for localized states the inverse participation ratio $\mathcal{R}_2$ is large while for delocalized states the IPR is small.

In practice, to obtain the IPR of a certain wave function, we have to sum its density function value squared, for every point of our space, or what is the same, the absolute value of the wave function ψ at every point raised to the fourth power.

$$\mathcal{R}_2 = \sum_i |\psi_i|^4 \tag{9.31}$$

where ψ_i denotes a discrete vector corresponding to the wave function $\psi(\mathbf{r})$.

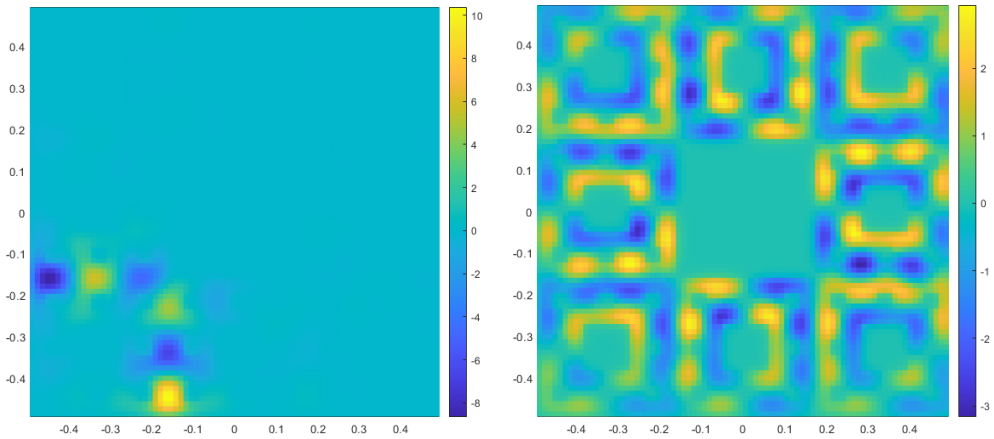

(a) $\mathcal{R}_2 = 37.78$, state number 53 (b) $\mathcal{R}_2 = 3.06$, state number 114

Figure 9.10: Wave functions with the highest and lowest IPR value between the first 1000 eigenstates of the particle in a box system, with potential with shape of Sierpinski carpet on its third iteration.

An important question to address is that of a possible localization. That is some states are extended over the system, so that the particle can propagate across the box, while other states are contained to a small region so that the particle remains effectively trapped and cannot escape. To graphically show what does it mean to have a wave function which is localized to a larger or a smaller extent, that if it has a greater IPR, we compute the first thousand quantum states of a system formed by a particle in a box, with zero boundary conditions and with an external potential with the shape of a Sierpinski carpet on its third iteration. We compute the IPR of each state and plot the ones with maximal and minimal IPR value.

Characteristic examples of the wave functions corresponding to large and small values of IPR are presented in Figure 9.10). The left panel (Fig. 9.10.a) shows the wave function of a localized state (i.e. with large IPR value). In this particular example, the particle gets localized in the lower-left corner. Contrary, the wave function of a delocalized state significantly extends over the available space in the box, as illustrated in Figure 9.10.b.

We searched for a relation between this IPR value and the energy of the quantum state, but no apparent relation was found.

9.9 Ground state wave function

In this section, we present some of the computed eigenvectors of the system. In Figure 9.11 we report the wave function obtained using the diagonalization method for the ground state of the system, for different iterations of the fractal using zero boundary conditions. The results obtained by using periodic boundary conditions are shown in Figure 9.12. Notice that, as we mentioned in the previous section, these states are the superposition of the degenerate states that occupy the same energy as the ground state.

It can be seen that the effect of a specific choice of the condition for the wave function at the borders of the box (zero or periodic boundary condition) strongly affects the ground state for small iterations (compare iterations 1,2,3 in Figures 9.11-9.12). Instead, for larger iteration numbers (compare iterations 4,5,6 in Figures 9.11-9.12) the effect of the boundary condition is not that important.

In Figure 9.13 we show how the ground state wave functions are modified when some random noise was applied to the potential. In absence of the random noise, the ground state is fourfold degenerate and the particle can be localized in any of the four angles or might stay in any linear combination of such states. The random noise lifts the degeneracy and the particle prefers to stay in only one corner, as it makes each state distinct and this way avoids the superposition of these degenerate states.

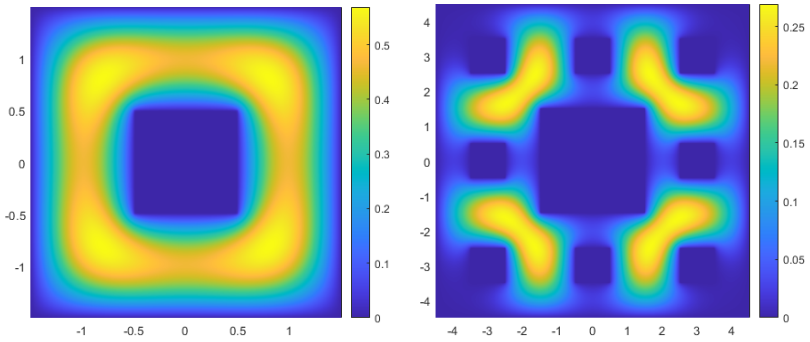

(a) Iteration 1

(b) Iteration 2

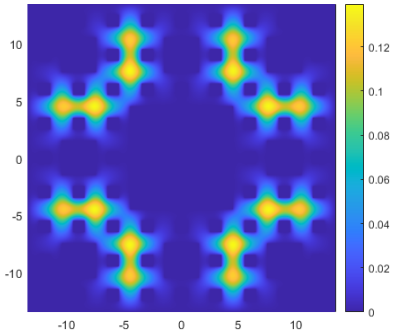

(c) Iteration 3

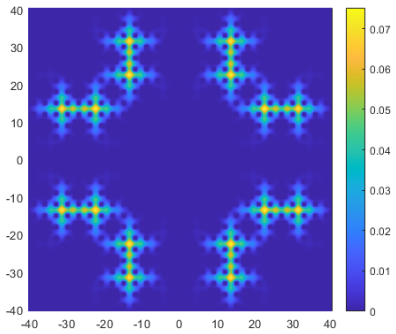

(d) Iteration 4

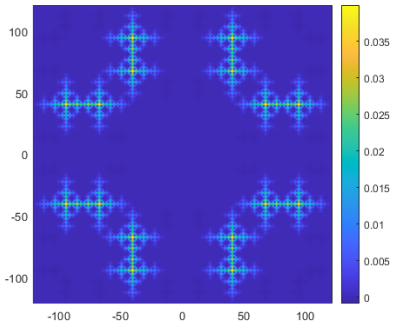

(e) Iteration 5

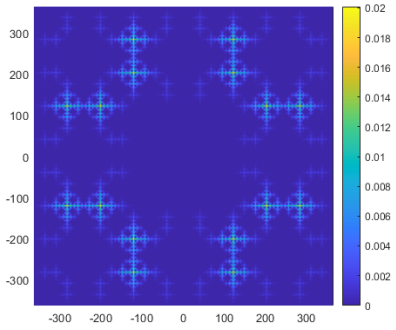

(f) Iteration 6

Figure 9.11: Color map of the wave functions of the first six lowest energy states of the system, for different iterations of the fractal, with zero boundary conditions. Blue regions, zero density, the least probable regions to find the particle. Yellow regions, larger density, the most probable regions to find the particle.

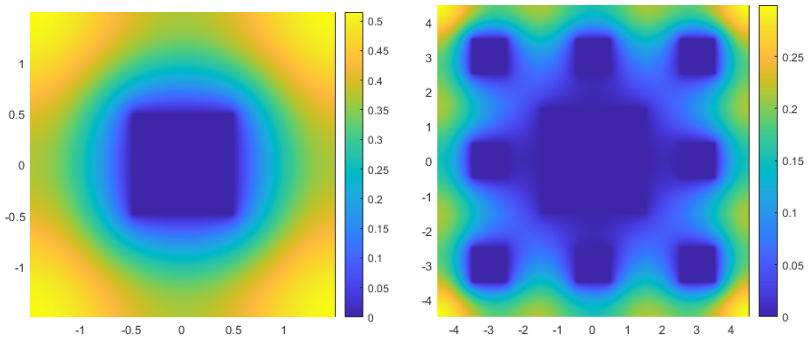

(a) Iteration 1

(b) Iteration 2

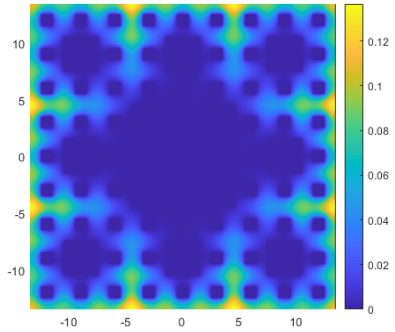

(c) Iteration 3

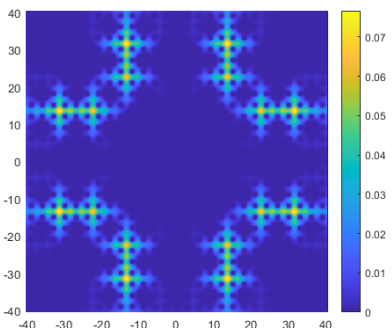

(d) Iteration 4

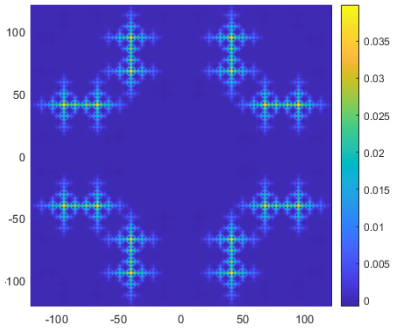

(e) Iteration 5

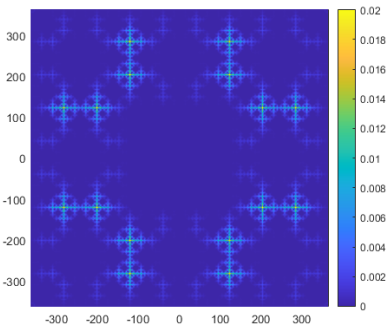

(f) Iteration 6

Figure 9.12: Color map of the wave functions of the first six lowest energy states of the system, for different iterations of the fractal, with periodic boundary conditions. Blue regions, zero density, the least probable regions to find the particle. Yellow regions, larger density, the most probable regions to find the particle.

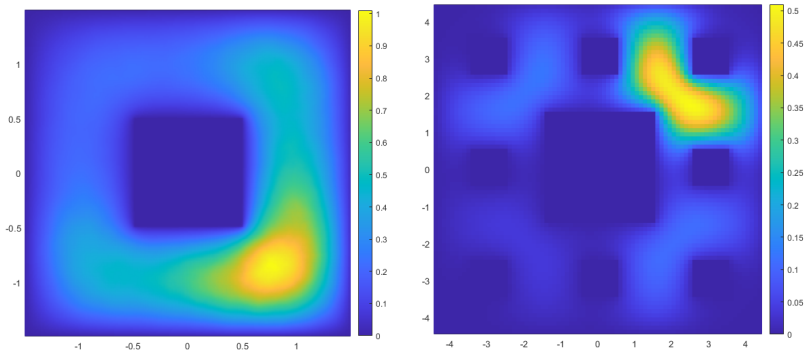

(a) Iteration 1, $\alpha = 60$

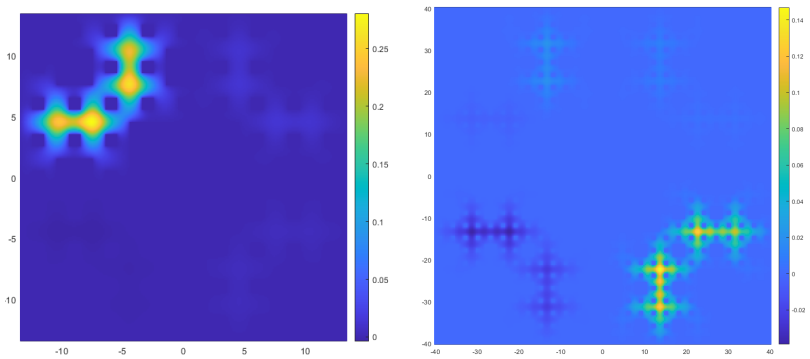

(b) Iteration 2, $\alpha = 1$

(c) Iteration 3, $\alpha = 0.1$

(d) Iteration 4, $\alpha = 0.025$

Figure 9.13: Color map of the wave functions of the first four lowest energy states of the system, for different iterations of the fractal, with zero boundary conditions. We applied some random noise α to the external potential to avoid superposition of degenerate states. Blue regions, zero density, the least probable regions to find the particle. Yellow regions, larger density, the most probable regions to find the particle.

9.10 Energy spectrum

An important quantity describing the energetic properties of the system is the energy spectrum, that is the eigenvalues of the Hamiltonian. An important question is how it evolves when increasing the iteration of the fractal. This eigenergies are obtained by computing eigenvalues of the Hamiltonian matrix that we exposed in the previous sections. In our discrete version of the problem, we can have up to N^2 quantum states with their respective eigenenergies.

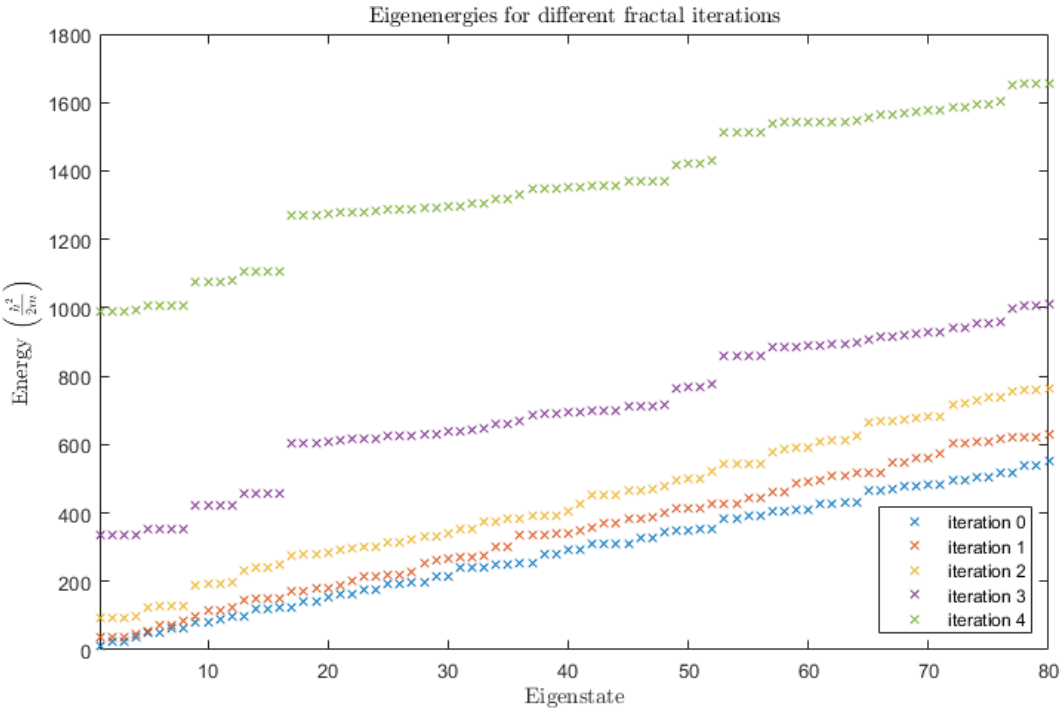

Figure 9.14: Energy of the lowest 80 eigenstates for different iterations of the fractal, with zero boundary conditions.

If we focus on the first 80 values of the energy spectrum, shown in Figure 9.14, we observe how a *band structure* is formed in the lowest eigenenergies. That is the energy levels bunch into small groups with very similar values, and there are gaps between one group and the next one. These groups are formed from degenerate states. For example, the ground state is fourfold degenerate with the corresponding wavefunctions shown in Figure 9.8. We find that the band structure is maintained when the fractal iteration increases, and it gets more accentuated, as the gaps between bands increase as well, following the exponential law presented in section 9.6.

But when we observe a bigger number of eigenvalues, we can see how this scaling law is replaced by a very similar curve among all iterations. This can be produced by the lack of needed precision due to discretization for those states. For this reason, we only assumed that the first 1000 values were accurate enough to work with on the next sections.

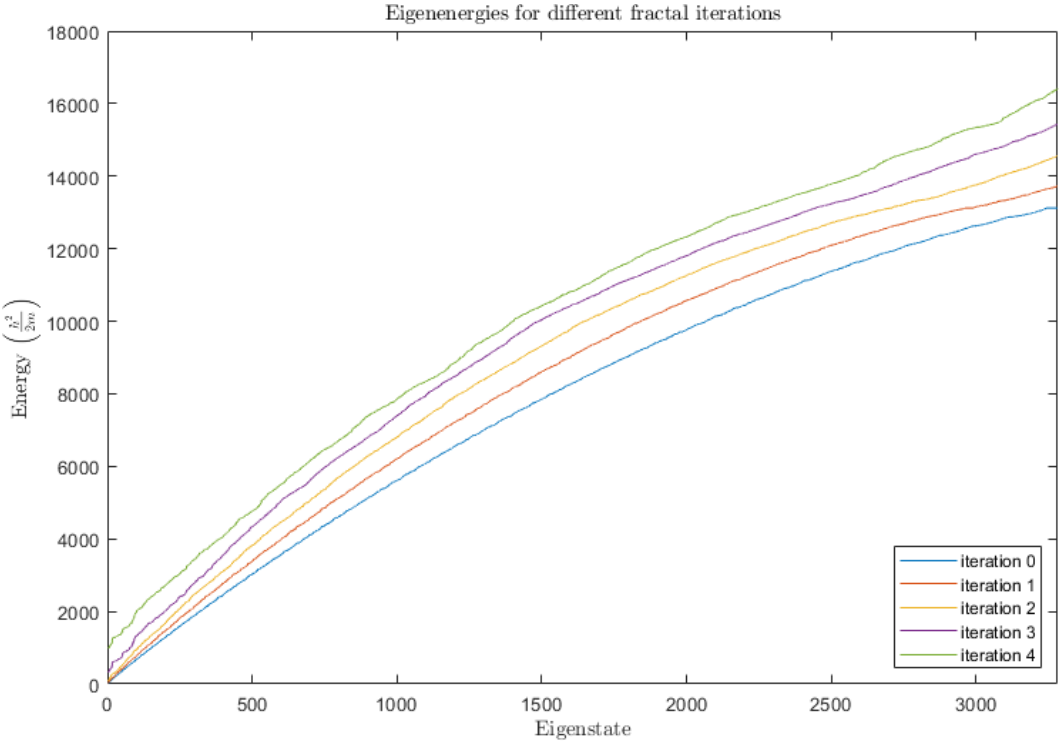

Figure 9.15: Energy of the eigenstates of the system for different iterations of the fractal, with zero boundary conditions

Something we observed was that when escalating the energy spectrum to compare states with the same energy of different fractal iterations, it seemed to disappear the gaps. These means that, instead of finding more states with the same or similar energy occupying the same bands as the previous iterations, these bands tended to diffuse, and a linear behavior could be seen, as we can see on Figure 9.16.

9.11 Comparing spectrum with different shaped potential

We previously compared the energy spectrum obtained by the Sierpinski carpet shaped external potential with the case where there is no potential at all. To extend this analysis, we defined a periodic external potential and computed the eigenvalues of it.

The periodic potential defined has a grid shape, similar to a chess grid, where one cell has potential and the next one is empty. We defined the iteration of this pattern y the number of cells it has on each row, being 2^i the number of cells per row on iteration i, as it can be seen on Figure 9.17.

We computed its spectrum and escalated the x coordinate, as we did on Figure 9.16, and we could observe a different behavior. On Figure 9.18 we see how for higher iterations of

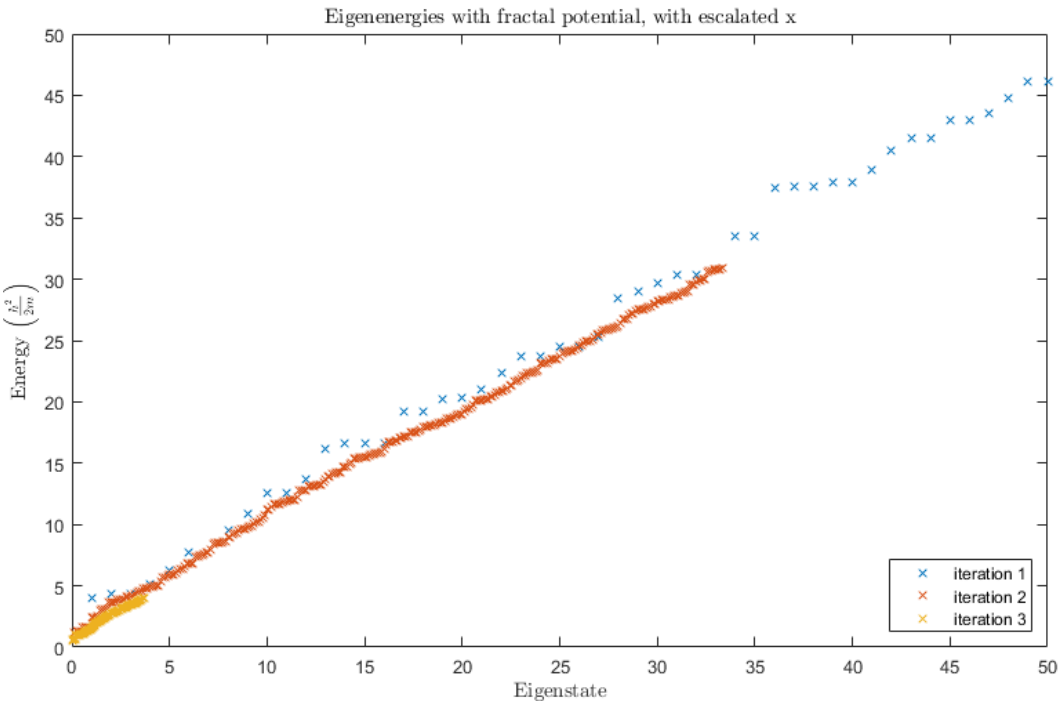

Figure 9.16: First 300 eigenvalues for iterations 1, 2 and 3 of the fractal. Values from iteration 2 and 3 are scaled so they match the energy values of iteration one.

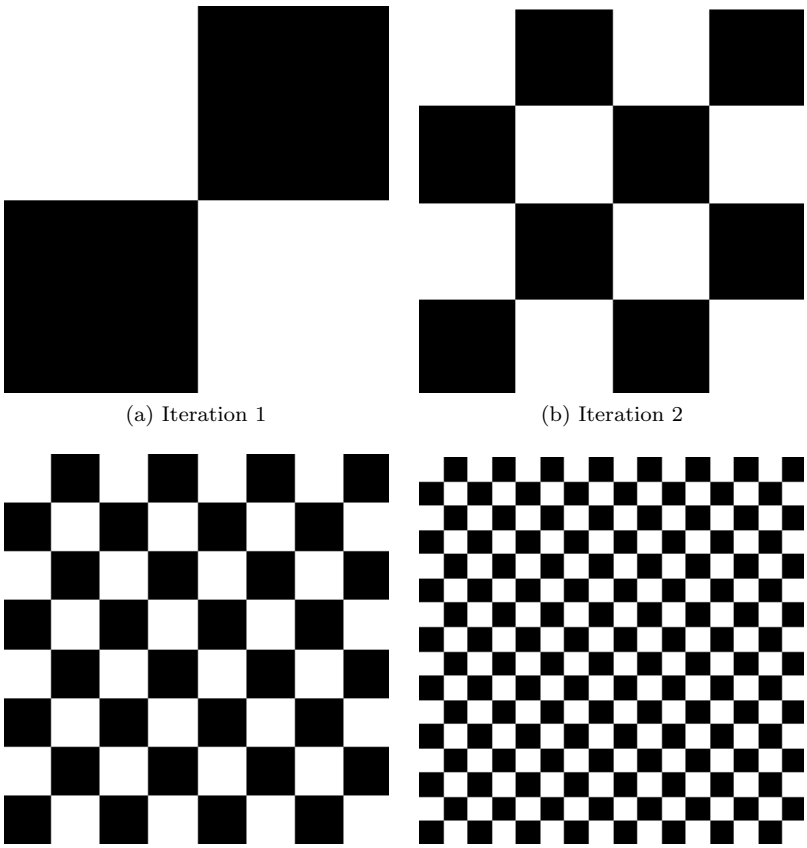

(a) Iteration 1 (b) Iteration 2

(c) Iteration 3 (d) Iteration 4

Figure 9.17: First four iterations of the periodic pattern that we use as external potential.

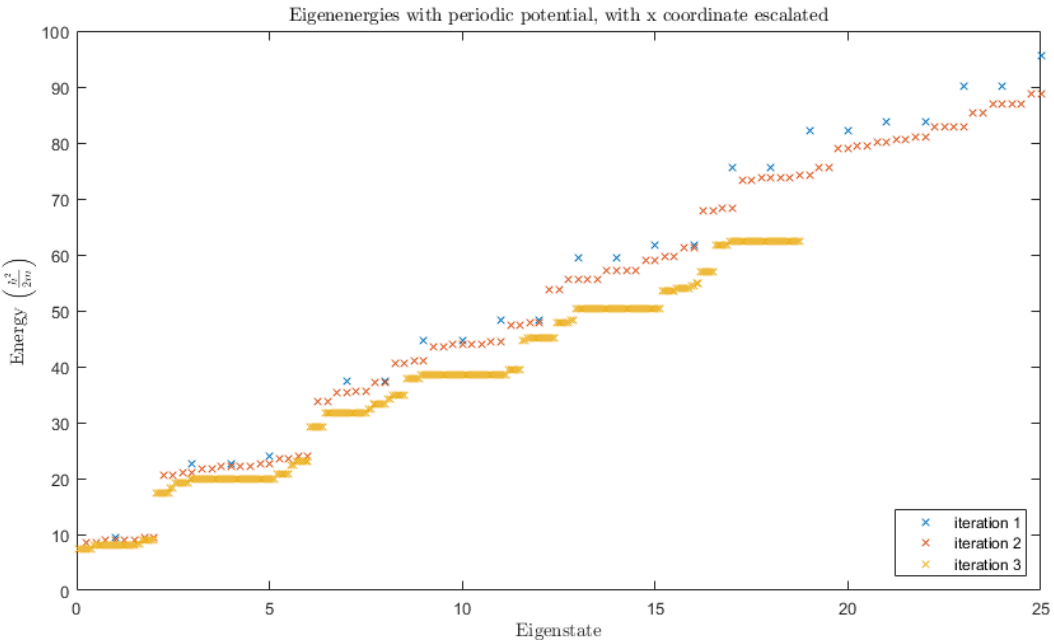

Figure 9.18: First 300 eigenvalues for iterations 1, 2 and 3 of the periodic potential. Values from iteration 2 and 3 are scaled, so they match the energy values of iteration one.

the potential, the gap seems to maintain, and the eigenvalues occupy the same bands as the previous iterations, but grouping way more states on each band.

To complete the analysis of the spectrum, we added Figure 9.19, where we computed the spectrum of the particle in a box system without any external potential. In the previous experiments for the periodic and the fractal potentials (Figure 9.16 and Figure 9.18), the physical length L escalated with the iteration, ensuring the minimum size of the potential was maintained constant. To match these experiments, we obtained the eigenvalues for different sizes of the system without external potential. This size is described by the parameter N, as we define a lattice space of $N \times N$, and the physical size of the box, which is equal to L.

On Figure 9.19 it can be clearly seen how in each iteration the gap between bands decreases, tending to a straight line when the discretization goes to infinity, where there is no prohibited energy values.

To conclude this section, we could say that the spectrum obtained with the fractal shaped potential falls between the periodic behavior, where the gap is maintained when increasing the iteration, and the zero potential behavior, where the gap is smaller when increasing the system's size, and tends to disappear on a continuous space.

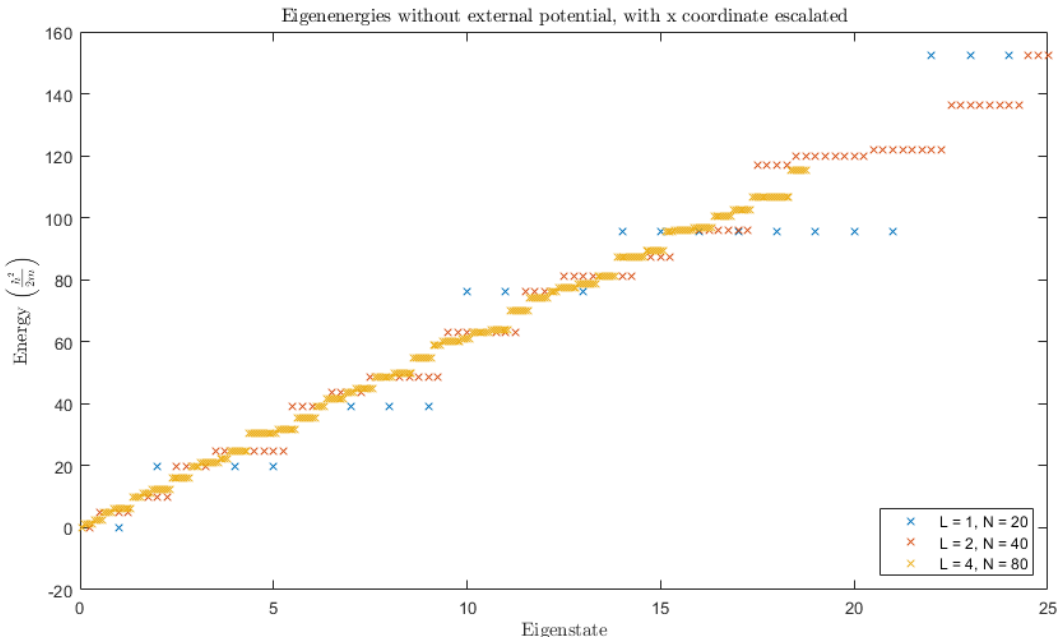

Figure 9.19: First 300 eigenvalues for particle in a box without external potential, for different sizes of the box. There is a scaling of the x coordinate so the values match.

Chapter 10

Time evolution of a quantum particle in Sierpinski carpet

All the work of the previous sections has been based on computing and observing the properties of stationary states, quantum states that are independent of time. Now, we are going to present a method that allows us to compute the wave function of a particle for a certain time value, or what is equivalent, the time evolution of a wave function. These means that we will be able to analyze properties which evolve with time, such as the time evolution of the wave packet describing the quantum particle.

10.1 Time-evolution of a quantum state

The Schrödinger equation looks as follows:

$$i\hbar\frac{\partial\psi(\mathbf{r},t)}{\partial t} = -\frac{\hbar^2}{2m}\nabla^2\psi(\mathbf{r},t) + V(\mathbf{r})\psi(\mathbf{r},t) \tag{10.1}$$

To separate the spatial and time dependencies, we factorize the wave function as $\psi(\mathbf{r},t) = \phi(\mathbf{r})f(t)$. With this in mind, we can replace ψ on the Schrödinger equation (10.1) and reorganize the terms in a way that we have all the time dependent parts in one side and the terms that depend on $\mathbf{r}$ on the other (10.2).

$$\frac{i\hbar}{f(t)}\frac{df}{dt} = \frac{1}{\phi(\mathbf{r})}\left[\frac{\hbar^2}{2m}\nabla^2 + V(\mathbf{r})\right]\phi(\mathbf{r}) \tag{10.2}$$

It can be seen how both sides must have the same value, that we could label with a constant E. This gives us the time-independent Schrödinger equation (10.3).

$$-\frac{\hbar^2}{2m}\nabla^2\phi(\mathbf{r}) + V(\mathbf{r})\phi(\mathbf{r}) = E\phi(\mathbf{r}) \tag{10.3}$$

$$\hat{\mathbf{H}}|\Psi\rangle = \mathbf{E}|\Psi\rangle \tag{10.4}$$

It also shows us that the temporal part of ψ can be rewritten as an exponential function, like we see on equation (10.6).

$$\frac{1}{f(t)}\frac{df(t)}{dt} = -\frac{iE}{\hbar} \tag{10.5}$$

$$f(t) = e^{-iEt/\hbar} \tag{10.6}$$

Putting the temporal part back together with $\phi(\mathbf{r})$, we can define ψ as:

$$\psi(\mathbf{r}, t) = \phi(\mathbf{r})e^{-iEt/\hbar} \tag{10.7}$$

On our previous section, we focused on solving the time-independent Schrödinger equation by obtaining the eigenvalues and eigenvectors of the discretized Hamiltonian operator. In our current notation, an eigenvector of this matrix would be a possible $\phi(\mathbf{r})$, and its correspondent eigenvalue would be the eigenenergy value E of that state. So by watching equation (10.7), with this eigenpairs computed, we could calculate the time-evolution of a quantum state of the system by just varying the value of t.

10.2 Superposition of eigen states

Notice how the $\psi(\mathbf{r}, \mathbf{t})$ obtained in equation (10.7) is just one possible solution to the Schrödinger equation and corresponds to a certain energy E. That is, the time evolution of the wave function $\phi_i(\mathbf{r}, t)$ of an eigenstate i corresponding to the energy E_i is

$$\phi_i(\mathbf{r}, t) = \phi_i(\mathbf{r})e^{-iE_it/\hbar} \tag{10.8}$$

The eigenstates form an orthonormal basis:

- each eigenstate is orthogonal to the others, that is for any eigenstates $i \neq j$

  $$\int \phi_i^*(\mathbf{r})\phi_j(\mathbf{r})\, d\mathbf{r} = 0 \tag{10.9}$$

  or in bra-ket notation, $\langle\phi_i|\phi_j\rangle = 0$

- each state can be considered normalized to unity

  $$\int \phi_i^*(\mathbf{r})\phi_i(\mathbf{r})\, d\mathbf{r} = 1 \tag{10.10}$$

  or in bra-ket notation, $\langle\phi_i|\phi_i\rangle = 1$

- any physical wave function $\Psi(\mathbf{r})$ can be expanded on the basis

  $$\psi(\mathbf{r}) = \sum_i c_i\phi_i(\mathbf{r}) \tag{10.11}$$

  where the (complex) coefficients c_i can be calculated as

  $$c_i = \int \phi_i^*(\mathbf{r})\psi(\mathbf{r})\, d\mathbf{r} \tag{10.12}$$

  or in bra-ket notation, $|\psi\rangle = \sum_i c_i|\phi_i\rangle$ and $c_i = \langle\phi_i|\psi\rangle$

- Condition that $\Psi(\mathbf{r})$ itself is normalized to unity is then

$$\sum_i |c_i|^2 = 1 \tag{10.13}$$

As according to Eq. (10.8) the time-evolution of each eigenfunction consists only in the evolution of the phase, the linear superposition of the wave function $\psi(\mathbf{r})$ in the zero moment of time as given by Eq. (10.11) actually defines the time-evolution for an arbitrary moment of time t, according to

$$\psi(\mathbf{r}, t) = \sum_i c_i \phi_i(\mathbf{r}) e^{-iE_i t/\hbar} \tag{10.14}$$

There is an infinite number of states in a quantum system, but as our system is discretized, we have a finite number of them. More precisely, our space is described as a lattice space of size $N \times N$ what let us compute a maximum number of N^2 eigenpairs, each one representing a quantum state. So, to obtain a solution of the Schrödinger as accurate as possible, we perform the linear combination of equation (10.14) with as many states as we can compute.

To obtain a wave function evolution, we need to specify the wave function state at $t = 0$. We will define this initial state as a two-dimensional Gaussian function, centered at the position (x_0, y_0) of the box:

$$\psi(\mathbf{r}, t = 0) = A \exp\left(-\frac{(x - x_0)^2}{2\sigma_x^2} - \frac{(y - y_0)^2}{2\sigma_y^2}\right) \tag{10.15}$$

For simplicity, we will have the same spread values for the x and y-axis, so $\sigma = \sigma_x = \sigma_y$.

10.3 Behaviour of displacement of the particle over time

It is interesting to notice that, to compute the time-evolution for a certain number of particles with different initial conditions, we do not have to perform the diagonalization method for each moment of time, as we can precompute the eigenvectors and eigenvalues of it and just load them on every execution. The only thing we have to recompute each time is the coefficient c_i of the expansion of the initial state on the eigenfunctions, but it is a pretty fast computation. Then one has just to compute the sum 10.14 over the eigenstates for each moment of time t, and obtain the resulting wave function $\psi(\mathbf{r}, t)$.

Taking these observations into account, we analyze the mean-square displacement of a particle on each time iteration, which is described as follows:

$$\text{MSD} \equiv \langle (\mathbf{x} - \mathbf{x}_0)^2 \rangle \tag{10.16}$$

As we compute $\psi(\mathbf{r}, t)$ for $\mathbf{r} = (x, y)$, we can obtain the MSD by evaluating the expected value of the operator on each time iteration:

$$\text{MSD(x, t)} = \int_{-\infty}^{\infty} \psi^*(x, y, t)(\mathbf{x} - \mathbf{x}_0)^2 \psi^*(x, y, t)\, dxdy \tag{10.17}$$

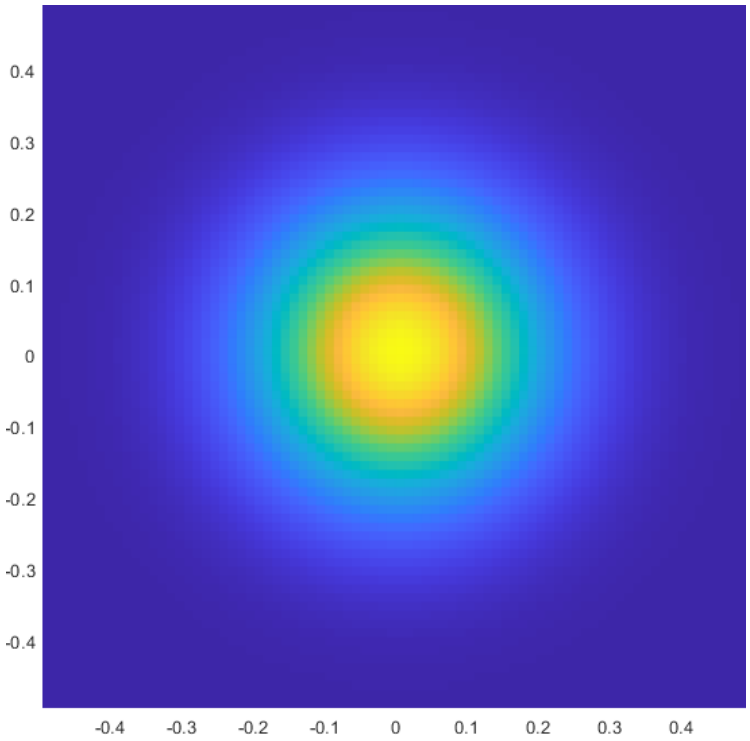

Figure 10.1: Initial wave function $\psi(\mathbf{r}, t = 0)$ defined by a two-dimensional Gaussian with $\sigma = 0.2$ and $A = 1$m centered at the origin.

In order to remove a possible dependence on the initial condition, we compute a large number of time evolutions, each one with an initial state wave function centered on a random position of the box. Then, we calculate the average mean-square displacement of each time iteration, for different iterations of the fractal shaped external potential, to compare the diffusion of a particle exposed to these different potentials.

The MSD time evolution of a free Gaussian wave packet should follow a ballistic expansion [8] described by the following equation:

$$\langle x^2 \rangle = \frac{\sigma^2}{2}\left[1 + \left(\frac{\hbar t}{m\sigma^2}\right)^2\right] \tag{10.18}$$

Indeed, we verify that the ballistic expansion explains the time evolution of MSD as shown in Figure 10.2 only for small time values, as for greater t values the borders of the box and of the fractal cause a rebound effect. It is interesting to see that this effect is perceived when MSD has not reached the box border, as opposed to a classical mechanics system, where the effect of the border is only present when it is reached.

Brownian motion of a particle, in which its position is randomly changed, in a free space leads to a linear time dependence of the MSD,

$$\langle x^2(t) \rangle \propto t, \tag{10.19}$$

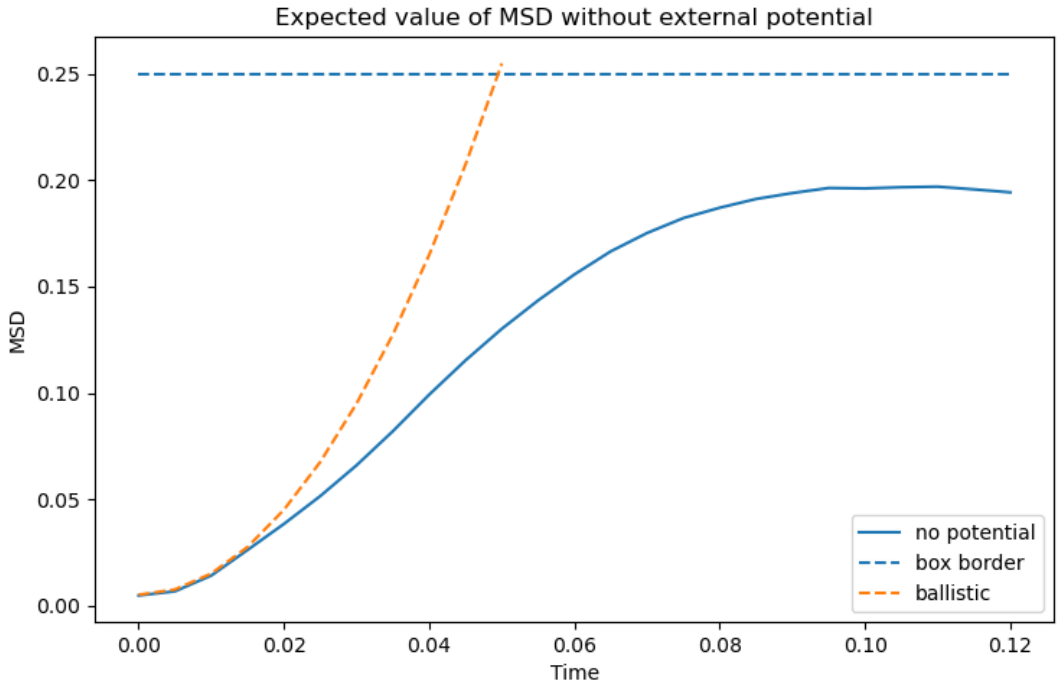

Figure 10.2: Average MSD of 300 executions, centering initial wave function randomly on the box, without external potential and with zero boundary conditions. The orange dashed line is a ballistic expansion. The blue dashed line is the border of the box.

and can be seen as a direct consequence of the central limit theorem. The linear relation (10.19) is known as the Einstein's diffusion relation. It was found in Ref. [9] that a diffusion in a discrete Sierpinski carpet (particle hops between squares of the minimal size) does not follow the usual Einstein's relation, $\langle x^2(t)\rangle \propto t$, but it rather follows an anomalous diffusion law[10],

$$\langle x^2(t)\rangle \propto t^{\gamma}, \tag{10.20}$$

where $0 < \gamma < 1$ is the diffusion exponent.

In Figure 10.3 we report the MSD time evolution for different iterations of the fractal. For small time values, when the particle has not get close to the minimum potential distance, which is equal $L/9^i$ being i the iteration of the fractal, the MSD increases as a ballistic expansion. But when it gets closer to the fractal edge, it produces a similar effect as the border of the box does on Figure 10.2, and starts following a diffusion law as seen on equation (10.20). This exponent γ decreases when we increase the iteration.

Something that we can also notice on Figure 10.3 is that, around $t = 0.8$, the wave function bounces on the edges of the box and starts going back to the middle, what leads to a decreasing MSD value.

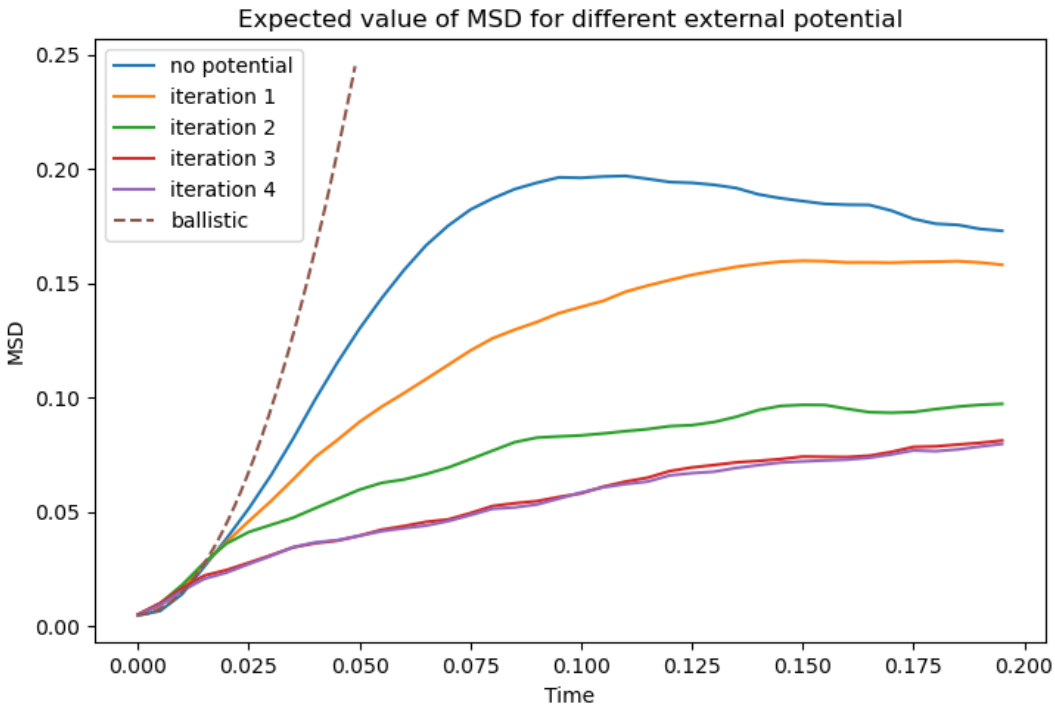

Figure 10.3: Average MSD of 300 executions, centering initial wave function randomly on the box, for different external potentials and with zero boundary conditions. The dashed line is a ballistic expansion.

Chapter 11

Conclusions

This thesis presents several valuable contributions for the study of quantum mechanics systems under the influence of an external potential with a fractal shape. We have implemented a program that can compute efficiently stationary states of a quantum system formed by a particle in a box, with zero or periodic boundary conditions, where you can set a custom external potential, with the desired shape, in our case a Sierpinski carpet fractal.

The second algorithm that we implemented lets you perform a superposition of the previously computed stationary states, and with it, you can obtain the general solution of the Schrödinger equation, or what is the same, a time evolution of the defined quantum system.

These two programs permit you to simulate the particle in a box system and to compute from it any property you are interested in. That is what allowed us to carry on a study analyzing the effects of applying this fractal shaped external potential to a certain quantum system.

We saw how the ground state energy of the system increased exponentially when increasing the iteration of the fractal. We could obtain this data thanks to the study of the best algorithm for computing the smallest eigenvalue of a matrix, as we computed it for matrices of size up to $43.046.721 \times 43.046.721$.

Another interesting conclusion of our static study is the analysis of the energy spectrum of this system, and how it varies when increasing the iteration of the fractal. We also performed a comparison between the spectrum of a system under the influence of a periodic potential, a fractal potential and a system without an external potential. From this comparison, we concluded that the periodic potential maintains its structure of bands when the shape of the box increases. The system without potential has fewer states per band, tending to a spectrum without any degenerate state when increasing the box's size. The system under the fractal potential felt in between of these two cases, as it maintains the band structure but the separation between bands decreases.

From our dynamic properties' analysis, we could verify how the time evolution of a free Gaussian wave packet follows a ballistic expansion, and visualized the effect of the boundary conditions. We also saw the diffusive behavior of the mean square displacement of a particle

on a fractal shaped external potential, and how it became more and more diffusive when increasing the iteration of the fractal.

Overall, we have achieved the initial objectives, which were the implementation of a program to solve numerically the Schrödinger equation, and the study of the properties of a certain quantum system, while relating them to the iteration of the fractal.

Furthermore, these programs can be fine-tuned to perform experiments with different shapes of external potential, different initial conditions or even a different quantum system, allowing all kinds of studies and experiments to emerge from this work.

Bibliography

[1] T Zoest, Naceur Gaaloul, Yeshpal Singh, Holger Ahlers, W Herr, Stephan Seidel, Wolfgang Ertmer, E Rasel, Michael Eckart, E Kajari, S Arnold, G Nandi, W.P. Schleich, R Walser, A Vogel, K Sengstock, Kai Bongs, W Lewoczko-Adamczyk, Max Schiemangk, and Jakob Reichel. Bose-einstein condensation in microgravity. *Science (New York, N.Y.)*, 328:1540–3, 06 2010.

[2] Jonathan O'Callaghan. Exotic fifth state of matter made on the international space station. *New Scientist*, 2020.

[3] Manifesto for Agile Software Development. `https://agilemanifesto.org/`. Accessed: 2021-03-15.

[4] Normativa del treball final de grau del grau en enginyeria informàtica de la facultat d'informàtica de barcelona. `https://www.fib.upc.edu/sites/fib/files/documents/estudis/normativa-tfg-mencio-addicional-gei-br.pdf`, 2020. Accessed: 2021-03-15.

[5] Taules retributives del personal docent i investigador laboral. `https://www.upc.edu/transparencia/ca/informacio-de-personal/sdg8_2_1_retribuciones_pdi_2020-1.pdf`, 2020. Accessed: 2021-03-15.

[6] Normativa del treball final de grau del grau en enginyeria informàtica de la facultat d'informàtica de barcelona. `https://www.fib.upc.edu/sites/fib/files/documents/estudis/normativa-tfg-mencio-addicional-gei-br.pdf`, 2021. Accessed: 2021-03-15.

[7] Amazon - lg gram 14z90n-v-aa78b. `https://www.amazon.es/LG-gram-14Z90N-V-AA78B-Ordenador-ultraligero/dp/B0861W8D24/`. Accessed: 2021-03-15.

[8] C. Jayaprakash. Problem: Evolution of a free gaussian wavepacket. `https://www.asc.ohio-state.edu/jayaprakash.1/631/freegauss.pdf`. Accessed: 2021-03-15.

[9] Karl Hoffmann, Michael Hofmann, Jens Lang, Gudula Rünger, and Steffen Seeger. Simulating anomalous diffusion on graphics processing units. pages 1 – 8, 05 2010.

[10] Ralf Metzler and Joseph Klafter. The random walk's guide to anomalous diffusion: A fractional dynamics approach. *Physics Reports*, 339:1–77, 12 2000.